

CHAPTER 1

INTRODUCTION

In modern power systems, apart from a large number of generators and associated controllers, there are many types of load, ranging from a simple resistive load to more complicated loads with electronic controllers. The influx of more and more controllers and loads, increase the complexity and nonlinearity of power systems. As a result power systems are viewed as complex nonlinear dynamical system that shows a number of instability problems. Instability problems in power systems that can lead to partial or full blackout can be broadly classified into three main categories, namely voltage, phase angle and frequency related problems.

The ability of synchronous machines of an interconnected power system to remain synchronism after being subjected to a small disturbance is known as small signal stability that is subclass of phase angle related instability problem. It depends on the ability to maintain equilibrium between electromagnetic and mechanical torques of each synchronous machine connected to power system. The change in electromagnetic torque of synchronous machine following a perturbation or disturbance can be resolved into two components – (i) a synchronizing torque component in phase with rotor angle deviation and (ii) a damping torque component in phase with speed deviation. Lack of sufficient synchronizing torque results in “aperiodic” or non-oscillatory instability, whereas lack of damping torque results in low frequency oscillations [1]

Low frequency oscillations are generator rotor angle oscillations having a frequency between 0.1 -2.0 Hz and are classified based on the source of the oscillation .The root cause of electrical power oscillations are the unbalance between power demand and available power at a period of time. In the earliest era of power system development, the power oscillations are almost non observable because generators are closely connected to loads, but nowadays, large demand of power to the farthest end of the system that forces to transmit huge power through a long transmission line, which results an increasing power oscillations.

The phenomenon involves mechanical oscillation of the rotor phase angle with respect to a rotating frame. Increasing and decreasing phase angle with a low frequency will be reflected in power transferred from a synchronous machine as phase angle is strong coupled to power transferred. The low frequency oscillations can be classified as local and inter-area mode.

1. Local modes are associated with the swinging of units at a generating station with respect to the rest of the power system. Oscillations occurred only to the small part of the power system. Typically, the frequency range is 1-2 Hz.
2. Interarea modes are associated with swinging of many machines in one part of the system against machines in other parts. It generally occurs in weak interconnected power systems through long tie lines. Typically frequency range is 0.1-1 Hz.

Besides these modes, there can be other modes associated with controllers which happen due to poor design of controllers. Torsional oscillation is another type of oscillation that happened in series capacitor compensated system and the frequency of oscillation is typically in sub synchronous frequency range. [2-3].

The traditional approach to address low frequency oscillation problem is to equip PSS in the machines which has tendency to damp out power oscillations. The basic function of a power system stabilizer is to extend stability limits by modulating generator excitation to provide damping to the oscillations of synchronous machine rotors relative to one another. These oscillations of concern typically occur in the frequency range of approximately 0.2 to 2.5 Hz, and insufficient damping of these oscillations may limit the ability to transmit power. To provide damping, the stabilizer must produce a component of electrical torque on the rotor which is in phase with speed variations. For any input signal the transfer function of the stabilizer must compensate for the gain and phase characteristics of the excitation system, the generator, and the power system, which collectively determine the transfer function from the stabilizer output to the component of electrical torque which can be modulated via excitation control.

Lightly damped oscillations can limit power transfer under weak system conditions, associated with either remote generation transmitting power over long distances or relatively weak inter ties connecting large areas. Stabilizer performance must therefore be measured in terms of enhancing damping under these weak system conditions. This measure must include not only the small-signal damping contributions to all modes of system oscillations but the impact upon system performance following large disturbances, when all modes of the system are excited simultaneously.

Based upon this measure, it is shown that the most appropriate stabilizer tuning criteria is to provide an adequate amount of damping to local modes of oscillation with a reasonably high contribution to Interarea modes of oscillation. Excess local mode damping is unnecessary and is often obtained at the expense of system performance following a large disturbance.

Stabilizers utilizing inputs of speed, power and frequency have been analyzed with respect to both tuning concepts and performance capabilities. Frequency has some inherent qualities which contribute to the desired performance criteria. However, any of these signals can be used to prevent oscillatory instabilities from limiting power transfer capability, at least to the point where other system considerations become limiting. Thus, the choice of input signal depends upon factors other than system performance alone [4-6].

However, the present power systems are too complex as many utilities around the world are interconnected each other to deliver reliable and cheap power from environmentally clean resources. Moreover, introduction of competition had invited many generating plants to be

connected to power system and started to dispatch power. Modern power systems are enormous and interconnected to serve large, remote load regions.

In recent years, voltage stability and voltage regulation have received wide attention. Voltage control, voltage regulation, reactive power Control, steady state stability etc. are important problems of power systems. Flexible AC Transmission Systems (FACTS) controllers can be used for solving these problems.

FACTS Controllers may be used to damp dynamic oscillations and increase damping of the swing modes. They improve damping by modulating the equivalent power-angle characteristic of the system. FACTS controllers are of two types – thyristor based and voltage sourced converter based. Static var compensator (SVC) and thyristor controlled series capacitor (TCSC) belong to the former category, while Static Compensator (STATCOM) and Unified power flow controller (UPFC) belong to the later.

SVC is a shunt FACTS Controller which is used for improvement of voltage profile of the transmission system. In addition, it also improves the transient stability of the system. SVC susceptance modulation using supplementary control signals in conjunction with the SVC voltage controller can be used to damp power system oscillations. Such supplementary signals can comprise rotor speed deviation, the active power deviation, line current etc. [7-18].

Fuzzy damping controllers have been reported [19-27] to be more effective in damping power system oscillations than conventional ones. Fuzzy Logic Controllers (FLC) is capable of tolerating uncertainty and imprecision to a greater extent so, they produce good results under changing operating conditions and uncertainties in system parameters. Fuzzy Logic based controller is likely to be an ideal choice for power system damping because of its adaptable nature. It is possible to design fuzzy logic controller by taking into account the non linearity of power system. It can be implemented easily because complicated and time consuming calculations are not involved.

In this work, a conventional and a fuzzy logic based SVC damping controller is developed for power oscillation damping. Different supplementary control signals have been adopted for both these controllers and the small signal stability of the system is studied. A comparison of the responses indicates that fuzzy logic based SVC damping controllers exhibit better performance characteristics than conventional ones.

CHAPTER 2

SMALL SIGNAL STABILITY OF A SINGLE MACHINE INFINITE BUS SYSTEM

2.1: Introduction

Small signal stability is the ability of the power system to maintain synchronism under small and slow disturbances such as gradual variation of load or slow increment of excitation. Parametric variation should not exceed by 5% under these small signal stability. Instability is of two form 1) steady increase in rotor angle due to lack of sufficient synchronizing torque. 2) Rotor oscillation of increasing amplitude due to lack of sufficient damping torque. The nature of system response to small disturbances depends on a no of factors including the initial operating point, the transmission system strength, and the type of generator excitations control used. For a generator connected radially to a large power system, in the absence of automatic voltage regulators (i.e with constant field voltage) the instability is due to lack of sufficient synchronizing torque. This result in instability through a non-oscillatory mode, whereas lack of damping torque results in low frequency oscillations With continuously acting voltage regulators, the small-disturbance stability problem is one of ensuring sufficient damping of system oscillations. In today's practical power system, small signal stability is largely a problem of insufficient damping of oscillations. The stability of the following types of oscillations is of concern:

- 1) Local modes or machine-system modes are associated with the swinging of units at a generating station with respect to the rest of the power system. The term local is used because oscillations are localized at one station or a small part of the power system.
- 2) Interarea modes are associated with the swinging of many machines in one part of the system against machines in other parts. They are caused by two or more groups of closely coupled machines being interconnected by weak ties.
- 3) Control modes are associated with generating unit and other controls. Poorly tuned exciters, speed governors, HVDC converters and static var compensators are the usual causes of instability of these modes.
- 4) Torsional modes are associated with the turbine-generator shaft system rotational components. Instability of torsional modes may be caused by interaction with excitation controls, speed governors, HVDC controls and series-capacitor-compensated lines.

Small-disturbance voltage stability is concerned with a system's ability to control voltages following small perturbations such as incremental change in system load. This form of stability is determined by the characteristic of load, continuous controls and discrete controls at a given instant of time. This concept is useful in determining, at any instant, how the system voltage will respond to small system changes.

The basic processes contributing to small-disturbance voltage instability are essential of a steady state nature. Therefore, static analysis can be effectively used to determine stability margins, identify factors influencing stability and examine a wide range of power system conditions. A criterion for small-disturbance voltage stability is that, at a given operating condition for every bus in the system, the bus voltage magnitude increases as the reactive power injection at the same bus is increased. A system is voltage-unstable if, for at least one bus in the system, the bus voltage magnitude (V) decreases as the reactive power injection (Q) at same bus is increased. In other words, a system is voltage-stable if V - Q sensitivity is positive for every bus and unstable if V - Q sensitivity is negative for at least one bus.

2.2: Characteristics of small-signal stability problems:

In large power systems, small-signal stability problems may be either local or global in nature.

2.2.1: Local problems

It involves a small part of the system. They may be associated with rotor angle oscillations of a single generator or a single plant against the rest of the power system. Such oscillations are called local plant mode oscillations. The stability problems related to such oscillations are similar to those of a single machine infinite bus system. Local problem may also be associated with oscillations between the rotors of few generators close to each other. Such oscillations are called intermachine or interplant mode oscillations. Usually, the local plant mode and interplant mode oscillations have frequencies in the range of 0.7-2.0 Hz.

Other possible local problems include instability of modes associated with controls of equipment such as generator excitation system, HVDC converters and static var compensators. The problems associated with control modes are due to inadequate tuning of the control system. In addition, these controls may interact with the dynamics of the turbine-generator shaft system, causing instability of torsional mode oscillations.

Analysis of local small-signal stability problems requires a detailed representation of a small portion of the complete interconnected power system. The rest of the system representation may be appropriately simplified by use of simple models and system equivalents. Usually, the complete system may be adequately represented by a model having several hundred states at most.

2.2.2: Global Problems

Global small-signal stability problems are caused by interactions among large group of generators and have widespread effects. They involve oscillations of a group of generators in one area swinging against a group of generators in another area. Such oscillations are called Interarea mode oscillations.

Large interconnected systems usually have two distinct forms of Interarea oscillations:

- a) A very low frequency mode involving all the generators in the system. The system is essentially split into two parts, with generators in one part swinging against machines in other part. The frequency of this mode of oscillation is on the order of 0.1-0.3 Hz.
- b) Higher frequency modes involving subgroups generators swinging against each other. The frequency of these oscillations is typically in the range of 0.4 to 0.7 Hz.

2.3: Power vs rotor angle relationship:

An important characteristic of power system stability is the relationship between interchange power and angular positions of the rotor of synchronous machine. This relationship is highly nonlinear. Let's consider two synchronous machines connected by a transmission line having a inductive reactance X_l but negligible resistance and capacitance. Let's assume that machine 1 represents a generator feeding power to a synchronous motor represented by machine 2. The power transferred from the generator to motor is a function of angular separation δ between the rotors of two machines. This angular separation is due to three components: generator internal angle (angle by which generator rotor leads the revolving field of stator); angular difference between the terminal voltages of generator and motor (angle by which the stator field of generator leads that of motor) and the internal angle of motor (angle by which rotor lags the revolving stator field. Power transferred from generator to motor is given by

$$P = (E_G * E_M * \sin\delta) / X_T$$

$$X_T = X_G + X_M + X_l$$

Here power varies as a sine of angle: a highly nonlinear relationship. When effect of automatic voltage regulator is considered, this power angle characteristic deviates significantly from its sinusoidal nature. When the angle is zero, no power is transferred. As angle is increased, the power transfer increases up to a maximum. After a certain angle, normally 90 degree, a further increase in angle results in a decrease in power transferred. There is thus a maximum steady state power that can be transferred between the two machines.

2.4: Effect of synchronous machine field circuit dynamics:

We consider the system performance including the effect of the field flux variations. The field voltage will be assumed constant (manual excitation control). We will develop the state-space model of the system by first reducing the synchronous machine equations to an appropriate form and then combining them with the network equations. We will express time in seconds, angles in electrical radians and all other variables in per unit.

2.4.1: Synchronous machine equations

The rotor angle is the angle (in electrical radian) by which the q-axis leads the reference E_B .

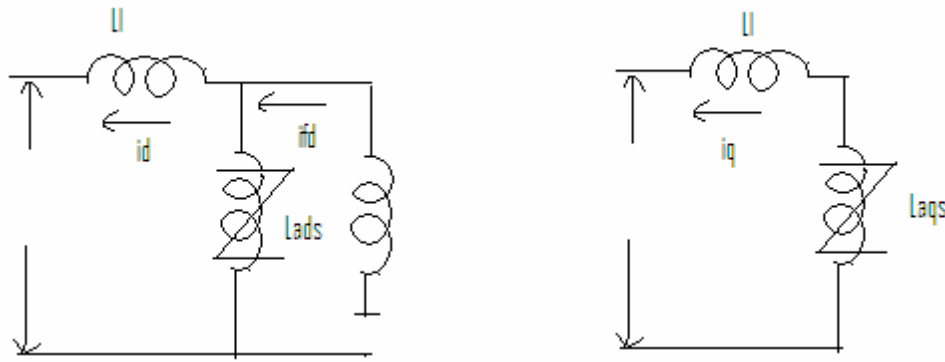


Figure 2.1: Equivalent circuit relating the machine flux linkages and currents

The stator and rotor flux linkages are given by

$$\varphi_d = -L_l i_d + L_{ads} (-i_d + i_{fd}) = -L_l i_d + \varphi_{ad} \quad (1)$$

$$\varphi_q = -L_l i_q + L_{aqs} (-i_q) = -L_l i_q + \varphi_{aq} \quad (2)$$

$$\varphi_{fd} = -L_{ads} (-i_d + i_{fd}) + L_{fd} i_{fd} = \varphi_{ad} + L_{fd} i_{fd} \quad (3)$$

In the above equations φ_{ad} and φ_{aq} are the air-gap (mutual) flux linkages and L_{ads} and L_{aqs} are the saturated values of mutual inductances.

From eqn, the field current may be expressed as

$$i_{fd} = \frac{\varphi_{fd} - \varphi_{ad}}{L_{fd}} \quad (4)$$

The d-axis mutual flux linkage can be written in terms of φ_{fd} and i_d as follows

$$\varphi_{ad} = -L_{ads} i_d + L_{ads} i_{fd} = -L_{ads} i_d + L_{ads} \left(\frac{\varphi_{fd} - \varphi_{ad}}{L_{fd}} \right)$$

$$\varphi_{ad} = L'_{ads} \left(-i_d + \left(\frac{\varphi_{fd}}{L_{fd}} \right) \right) \quad (5)$$

$$\text{Where, } L'_{ads} = \frac{1}{\frac{1}{L_{ads}} + \frac{1}{L_{fd}}} \quad (6)$$

Since there is no rotor circuits considered in the q-axis, the mutual flux linkage is given by

$$\varphi_{aq} = L_{aqs}(-i_q) \quad (7)$$

The air-gap torque is,

$$T_e = \varphi_d i_q - \varphi_q i_d = \varphi_{ad} i_q - i_d \varphi_{aq} \quad (8)$$

With speed variations neglected the stator voltage equations become,

$$e_d = -R_a i_d - \varphi_q \quad (9)$$

$$e_q = -R_a i_q - \varphi_d \quad (10)$$

2.4.2: Network equations

Since there is only one machine, the machine as well as network equations can be expressed in terms of one reference frame, i.e. the d-q reference frame of the machine. The machine terminal and infinite bus voltages in terms of the d and q components are

$$E_t = e_d + j * e_q \quad (11)$$

$$E_b = E_{bd} + j * E_{bq} \quad (12)$$

The network constraint equation for the system is

$$E_t = E_b + (R_e + j * X_e) * I_t \quad (13)$$

$$e_d + j * e_q = E_{bd} + j * E_{bq} + (R_e + j * X_e) * (i_d + j * i_q) \quad (14)$$

Resolving into d and q components gives

$$e_d = R_e i_d - X_e i_q + E_{bd} \quad (15)$$

$$e_q = R_e i_q - X_e i_d + E_{bq} \quad (16)$$

$$E_{bd} = E_b \sin \delta \quad (17)$$

$$E_{bq} = E_b \cos \delta \quad (18)$$

Using equations and to eliminate e_d , e_q in equations and using the expressions for φ_{ad} and φ_{aq} given by equations and, we obtain the following expressions for i_d and i_q in terms of state variables φ_{fd} & δ .

$$i_d = \frac{\left[X_{tq} \left\{ \varphi_{fd} \left(\frac{L_{ads}}{L_{ads} + L_{fd}} \right) - E_b \cos \delta \right\} - R_T E_b \sin \delta \right]}{D} \quad (19)$$

$$i_q = \frac{\left[R_T \left\{ \varphi_{fd} \left(\frac{L_{ads}}{L_{ads} + L_{fd}} \right) - E_b \cos \delta \right\} - X_{Td} E_b \sin \delta \right]}{D} \quad (20)$$

$$R_T = R_a + R_e \quad (21)$$

$$X_{tq} = X_e + (L_{aqs} + L_l) \quad (22)$$

$$X_{Td} = X_e + (L'_{ads} + L_l) \quad (23)$$

$$D = R_T^2 + X_{tq} X_{Td} \quad (24)$$

The reactances X_{qs} and X_{ds}' are saturated values. In per unit they are equal to the corresponding inductances.

2.4.3: Linearized system equations

Expressing equations and in terms of perturbed values, we may write

$$\Delta i_d = m_1 \Delta \delta + m_2 \Delta \varphi_{fd} \quad (25)$$

$$\Delta i_q = n_1 \Delta \delta + n_2 \Delta \varphi_{fd} \quad (26)$$

$$m_1 = \frac{E_b * (X_{tq} \sin \delta_0 - R_T \cos \delta_0)}{D}$$

$$n_1 = \frac{E_b * (R_T \sin \delta_0 - X_{Td} \cos \delta_0)}{D}$$

$$m_2 = \frac{X_{tq}}{D} * \left(\frac{L_{ads}}{L_{ads} + L_{fd}} \right)$$

$$n_2 = \frac{R_T}{D} * \left(\frac{L_{ads}}{L_{ads} + L_{fd}} \right) \quad (27)$$

By linearizing equations (5) and (7) and substituting in them the above expressions for i_d & i_q . we get

$$\Delta\varphi_{ad} = L'_{ads} \left(-\Delta i_d + \left(\frac{\Delta\varphi_{fd}}{L_{fd}} \right) \right) = \left(\frac{1}{L_{fd}} - m_2 \right) L'_{ads} \Delta\varphi_{fd} - m_2 L'_{ads} \Delta\delta \quad (28)$$

$$\Delta\varphi_{aq} = -n_2 L_{aqs} \Delta\varphi_{fd} - n_1 L_{aqs} \Delta\delta \quad (29)$$

Linearizing equation (4) and substituting for $\Delta\varphi_{fd}$ from equation (28) gives

$$\Delta i_{fd} = \frac{\Delta\varphi_{fd} - \Delta\varphi_{ad}}{L_{fd}} = \frac{1}{L_{fd}} * \left(1 - \left(\frac{L'_{ads}}{L_{fd}} \right) + m_2 L'_{ads} \right) \Delta\varphi_{fd} + \frac{1}{L_{fd}} * m_1 L'_{ads} \Delta\delta \quad (30)$$

The linearized form of equation (8) is

$$\Delta T_e = \varphi_{ado} \Delta i_q + i_{qo} \Delta\varphi_{ad} - \varphi_{aqo} \Delta i_d - i_{do} \Delta\varphi_{aq}$$

Substituting for $\Delta i_d, \Delta i_q, \Delta\varphi_{ad}, \Delta\varphi_{aq}$ from equations (25) to (29), we obtained

$$\Delta T_e = K_1 \Delta\delta + K_2 \Delta\varphi_{fd} \quad (31)$$

$$\text{Where , } K_1 = n_1 (\varphi_{ado} + L_{aqs} i_{do}) - m_1 (\varphi_{aqo} + L'_{ads} i_{qo}) \quad (32)$$

$$K_2 = n_2 (\varphi_{ado} + L_{aqs} i_{do}) - m_2 (\varphi_{aqo} + L'_{ads} i_{qo}) + \left(\frac{L'_{ads}}{L_{fd}} \right) * i_{qo} \quad (33)$$

By using the expressions for Δi_{fd} and ΔT_e given by equations (30) and (31), we obtain the system equations in the desired final form:

$$\begin{bmatrix} \Delta \dot{w}_r \\ \Delta \dot{\delta} \\ \Delta \dot{\varphi}_{fd} \end{bmatrix} = \begin{bmatrix} a_{11} & a_{12} & a_{13} \\ a_{21} & 0 & 0 \\ 0 & a_{32} & a_{33} \end{bmatrix} * \begin{bmatrix} \Delta w_r \\ \Delta \delta \\ \Delta \varphi_{fd} \end{bmatrix} + \begin{bmatrix} b_{11} & 0 \\ 0 & 0 \\ 0 & b_{32} \end{bmatrix} \begin{bmatrix} \Delta T_m \\ \Delta E_{fd} \end{bmatrix} \quad (34)$$

Where

$$a_{11} = -\frac{K_D}{2H}$$

$$a_{12} = -\frac{K_1}{2H}$$

$$\begin{aligned}
a_{13} &= -\frac{K_2}{2H} \\
a_{21} &= w_0 \\
a_{32} &= -\frac{w_0 m_1 L'_{ads} R_{fd}}{L_{fd}} \quad \& \\
a_{33} &= -\frac{w_0 R_{fd}}{L_{fd}} \left(1 - \left(\frac{L'_{ads}}{L_{fd}} \right) + m_2 L'_{ads} \right) \\
b_{11} &= \frac{1}{2H} \\
b_{32} &= \frac{w_0 R_{fd}}{L_{adu}}
\end{aligned}$$

And ΔT_m and ΔE_{fd} depend on prime-mover and excitation controls. With constant mechanical input torque, $\Delta T_m=0$; with constant exciter output voltage, $\Delta E_{fd}=0$.

The mutual inductances L_{ads} and L_{aqs} in the above equations are saturated values.

2.4.4: Field circuit effect

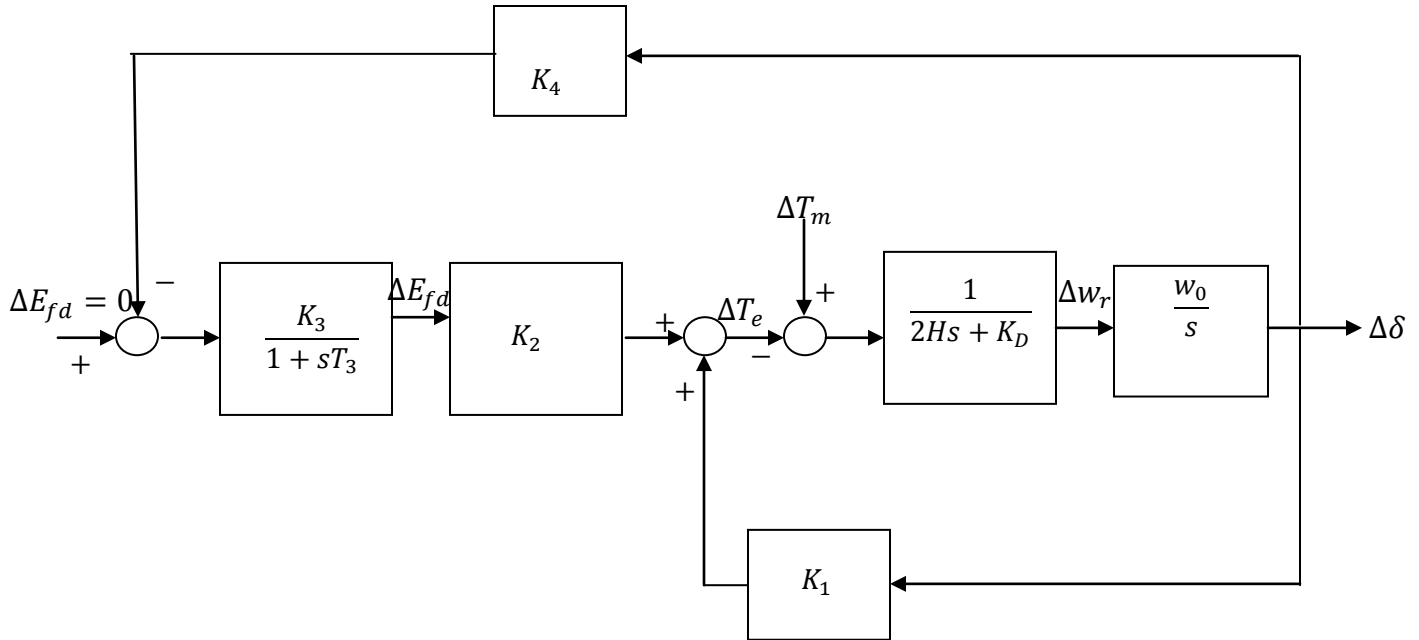


Figure 2.2: Block diagram representation with constant E_{fd}

From equation (31), Air-gap torque is expressed as a function of $\Delta\delta$ and $\Delta\varphi_{fd}$,

$$i.e \Delta T_e = K_1\Delta\delta + K_2\Delta\varphi_{fd}$$

Where ,

$$K_1 = \frac{\Delta T_e}{\Delta\delta} \text{ With constant } \varphi_{fd}$$

$$K_2 = \frac{\Delta T_e}{\Delta\varphi_{fd}} \text{ With constant rotor angle } \delta$$

The expression for K_1 and K_2 are given by equations (32) & (33). The component of torque given by $K_1\Delta\delta$ is in phase with $\Delta\delta$ and hence represent a synchronizing torque component and the component of torque resulting from variations in field flux linkage is given by $K_2\Delta\varphi_{fd}$. The variation of φ_{fd} is determined by the field circuit dynamic equation:

$$\Delta\dot{\varphi}_{fd} = a_{32}\Delta\delta + a_{33}\Delta\varphi_{fd} + b_{32}\Delta E_{fd} \quad (35)$$

As from the block diagram of fig (2.2)

$$\Delta\varphi_{fd} = \frac{K_3}{(1+sT_3)} [\Delta E_{fd} - K_4\Delta\delta] \quad (36)$$

Comparing equations (35) & (36) we get,

$$K_3 = -b_{32}/a_{33}, K_4 = -a_{32}/b_{32}, T_3 = -1/a_{33}$$

2.4.5: Effect of field flux linkage variation on system stability

From block diagram of fig (a), It is seen that, with constant field voltage ($\Delta E_{fd} = 0$), the field flux variations are caused only by feedback of $\Delta\delta$ through the co-efficient K_4 . This represents the demagnetizing effect of the armature reaction. The change in air-gap torque due to field flux variations caused by rotor angle change is given by

$$\frac{\Delta T_e}{\Delta\delta} (\text{due to } \Delta\varphi_{fd}) = -K_3K_4K_2/(1 + sT_3) \quad (37)$$

The constant K_3, K_4, K_2 are usually positive. The contribution of $\Delta\varphi_{fd}$ to synchronizing and damping torque components depends on the oscillating frequency as discussed below.

- a) In the steady state and at very low oscillating frequencies ($s=j\omega$ stands to 0):

$$\Delta T_e (\text{due to } \Delta\phi_{fd}) = -K_3 K_4 K_2 \Delta\delta$$

The field flux variation due to $\Delta\delta$ feedback (i.e, due to armature reaction) introduces a negative synchronizing torque component. The system becomes monotonically unstable when this exceeds $K_1\Delta\delta$. The steady-state stability limit is reached when,

$$K_1 = K_3 K_4 K_2$$

- b) At oscillating frequency much higher than $1/T_3$

$$\Delta T_e \approx -K_3 K_4 K_2 \Delta\delta / j\omega T_3$$

$$\Delta T_e = K_3 K_4 K_2 j \Delta\delta / \omega T_3$$

Thus, the component of air-gap torque due to $\Delta\phi_{fd}$ is 90 degree ahead of $\Delta\delta$ or in phase with $\Delta\omega$. Hence, $\Delta\phi_{fd}$ results in a positive damping torque component.

- c) At typical machine oscillating frequencies of about 1 Hz (2π rad/sec), $\Delta\phi_{fd}$ results in a positive damping torque component and a negative synchronizing torque component. The net effect is to reduce slightly the synchronizing torque component and increase the damping torque component.

The coefficient K_4 is normally positive. As long as it is positive, the effect of field flux variation due to armature reaction is to introduce a positive damping torque component. However, there can be situation where K_4 is negative. As K_4 is proportional to the term ' $(X_{tq} \sin\delta_0 - R_T \cos\delta_0)$ ', so K_4 is negative when ' $(X_{tq} \sin\delta_0 - R_T \cos\delta_0)$ ' is negative. This is the situation when a hydraulic generator without damper winding is operating at light load and is connected by a line of relatively high resistance to reactance ratio to a large system. Also K_4 can be negative when a machine is connected to a large local load, supplied partly by the generator and partly by the remote large system. Under such conditions, the torques produced by induced currents in the field due to armature reaction has components out of phase with $\Delta\omega$, and produce negative damping.

2.5: Power system stabilizer

2.5.1: Introduction

Power system stabilizers have been applied to generator excitation systems to aid damping of power system electromechanical oscillations since the mid-1960. The basic function of a power system stabilizer is to extend stability limits by modulating generator excitation to provide damping to the oscillations of synchronous machine rotors relative to one another. These oscillations of concern typically occur in the frequency range of approximately 0.2 to 2.5 Hz, and insufficient damping of these oscillations may limit the ability to transmit power.

To provide damping, the stabilizer must produce a component of electrical torque on the rotor which is in phase with speed variations. For any input signal the transfer function of the stabilizer must compensate for the gain and phase Characteristics of the excitation system, the generator, and the power system, which collectively determine the transfer function from the stabilizer output to the component of electrical torque which can be modulated via excitation control.

The objective of power system stabilizers is to extend stability limits on power transfer by enhancing damping of system oscillations via generator excitation control. Lightly damped oscillations can limit power transfer under weak system conditions, associated with either remote generation transmitting power over long distances or relatively weak inter ties connecting large areas. Stabilizer performance must therefore be measured in terms of enhancing damping under these weak system conditions. This measure must include not only the small-signal damping contributions to all modes of system oscillations but the impact upon system performance following large disturbances, when all modes of the system are excited simultaneously.

Based upon this measure, it is shown that the most appropriate stabilizer tuning criteria is to provide an adequate amount of damping to local modes of oscillation with a reasonably high contribution to Inter area modes of oscillation. Excess local mode damping is unnecessary and is often obtained at the expense of system performance following a large disturbance. Stabilizers utilizing inputs of speed, power, and frequency have been analyzed with respect to both tuning concepts and performance capabilities. Frequency has some inherent qualities which contribute to the desired performance criteria. However, any of these signals can be used to prevent oscillatory instabilities from limiting power transfer capability, at least to the point where other system considerations become limiting. Thus, the choice of input signal depends upon factors other than system performance alone.

If the exciter transfer function $G_{ex}(s)$ and the generator transfer function between ΔE_{fd} and ΔT_e were pure gains, a direct feedback of $\Delta \omega_r$ would result in a damping torque component. However in practice both generator and exciter exhibit frequency dependent gain and phase characteristics. Therefore, the PSS transfer function; $G_{pss}(s)$ should have phase compensation circuit to compensate for the phase lag between the exciter input and the electrical torque.

In the ideal case, with the phase characteristic of $G_{pss}(s)$ being an exact inverse of the exciter and generator phase characteristics to be compensated, the PSS would result in a pure damping torque at all oscillating frequencies.

2.5.2: PSS composition

The PSS consists of three blocks: a phase compensation block, a signal washout block, and a gain block.

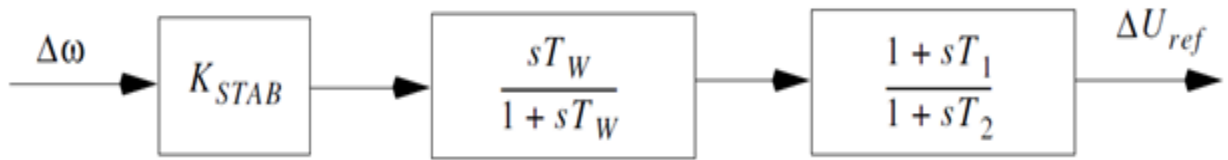


Figure 2.3: PSS structure

The phase compensation block provides the appropriate phase-lead characteristic to compensate for the phase lag between the exciter input and the generator electrical torque. The phase-lead network should provide compensation over the frequency range of 0.1 to 2.0 Hz. The phase characteristic to be compensated changes with the system condition; therefore a compromise is made and a characteristic acceptable for different system condition is selected. Generally some under compensation is desirable so that the PSS, in addition to increase the damping torque, results in a slight increase of synchronizing torque.

The signal washout block serves as a high pass filter, with the time constant high enough to allow signals associated with oscillation in w_r to pass unchanged. Without it, steady changes in speed would modify the terminal voltage. It allows the PSS to respond only to changes in speed. From the viewpoint of its function, the value of time constant is not critical and may be in the range of 1 to 20 seconds.

The stabilizer gain determines the amount of damping introduced by the PSS. Ideally, the gain should be set at a value corresponding to maximum damping; however it is often limited by other considerations. In applying the PSS, care should be taken to ensure that the overall stability is enhanced, not just small signal stability.

2.5.3: Selection of PSS parameters

1. Maximize the damping of the local plant mode as well as inter-area mode oscillations without compromising the stability of other modes.
2. Enhance system transient stability.
3. Not adversely affect system performance during major system upsets which cause large frequency excursions.
4. Minimize the consequences of excitation system malfunction due to component failures.

CHAPTER 3

FACTS CONTROLLER

Transmission systems are becoming increasingly stressed because of growing demand and because of restrictions on building new lines. However, most high voltage transmission systems are operating below their thermal rating due to such constraints as stability limits. EPRI is pioneering flexible ac transmission system (FACTS) technology to make it possible to load lines at least for some contingencies up to their thermal limits without compromising system reliability. Modern power systems are enormous and interconnected to serve large, remote load regions. In recent years, voltage stability and voltage regulation have received wide attention. Voltage control, voltage regulation, reactive power control, steady state stability etc. are important problems of power systems. Flexible AC Transmission Systems (FACTS) controllers can be used for solving these problems.

Power system damping controllers such as power system stabilizer (PSS) and FACTS based stabilizers may be used to damp dynamic oscillations and increase damping of the swing modes. PSS increases damping torque of a generator by affecting the generator excitation control, while facts devices improve damping by modulating the equivalent power-angle characteristic of the system. Dynamic application of FACTS controllers includes dynamic stability, voltage stability enhancement and transient stability improvement. Among FACTS controllers, the shunt controllers have shown feasibility in term of cost effectiveness in a wide range of problem-solving from transmission to distribution levels. In principle, all shunt-type controllers inject additional current into the system at the point of common coupling.

3.1: SVC (Static VAR Compensator)

3.1.1: Introduction and connection

The SVC is the most widely used FACTS device in power system regulation. It usually installs in power transmission systems and serves in various ways to improve the system performance. The damping obtained depends on SVC location in the system and its control signal. It has been found that the mid-point of the transmission circuit, connecting the two oscillating groups of machines in the iter-area mode is the best SVC location for damping enhancement. An SVC can alter the $P - \delta$ curve by changing its output B_{SVC} (suceptance) in such a way that damping is increased. For example, for a one machine infinite bus system, if the speed deviation of the machine is fed back as supplementary signal to the SVC input, then B_{SVC} and subsequently the $P - \delta$ curve, will be altered such that the speed deviation is decreased and therefore, damping can be increased.

We use either tie-line active power signal or speed difference signal as input to the SVC for damping Inter area modes. SVC is an effective and economical means of solving problems of transient stability, system reliability, static voltage stability, dynamic stability and steady state stability in long transmission lines. Static VAR Compensator (SVC) was first introduced in late 1960s. SVC is used to improve voltage profile primarily. It can also be used to improve steady state stability limit. It can improve small signal stability when supplementary control with auxiliary signals are used, as in this paper, it is shown with auxiliary signal as rotor speed and line current separately.

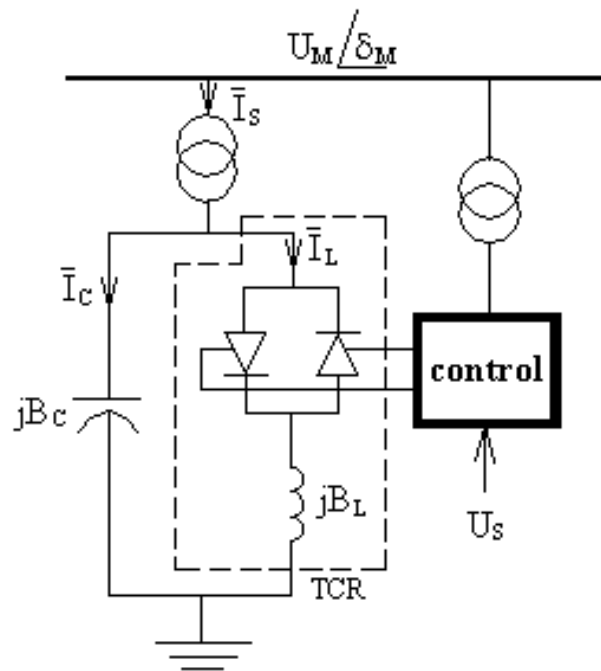


Figure 3.1: SVC connection diagram

SVC is basically a shunt connected static var generator whose output is adjusted to exchange capacitive (I_c) or inductive current (I_L) so as to maintain or control specific power variable; typically, the control variable is the SVC bus voltage (U_M). One of the major reason for installing a SVC is to improve dynamic voltage control and thus increase system loadability. There are the mainly accomplishes work to construct an effective for SVC. Firstly, to design a controller for SVC devices on transmission lines, a Single Machine Infinite Bus (SMIB) system is modeled. A stated space mathematical model is constructed. SVC is thyristor based controller that provides rapid voltage control to support electric power transmission voltages during immediately after major disturbances.

Since the advent of deregulation and the separation of generation and transmission systems in electric industry, voltage stability and reactive power-related system restrictions have become an

increasing growing concern for electric utilities. The SVC provides an excellent source of rapidly controllable reactive shunt compensation for dynamic voltage control through its utilization of high-speed thyristor switching/controlled reactive devices.

Generally, static VAR compensation is not done at line voltage; a bank of transformers steps the transmission voltage (for example, 230 kV) down to a much lower level (for example, 9.5 kV). This reduces the size and number of components needed in the SVC, although the conductors must be very large to handle the high currents associated with the lower voltage.

An SVC is typically made up of the following major components:

1. Coupling transformer
2. Thyristor valves
3. Reactors
4. Capacitors (often tuned for harmonic filtering)

In general, the two thyristor valve controlled/switched concepts used with SVCs are the thyristor-controlled reactor (TCR) and the thyristor-switched capacitor (TSC). The TSC provides a “stepped” response and the TCR provides a “Smooth” or continuously variable susceptance.

A TCR/FC including the operating process concept.

3.1.2: SVC V-I Characteristic

The control objective of SVC is to maintain the desired voltage at a high voltage bus. In steady-state, the SVC will provide some steady-state control of the voltage to maintain it the highest voltage bus at the pre-defined level. If the voltage bus begins fall below its setpoint range, the SVC will inject reactive power (Q_{net}) into the system (within its control limits), thereby increasing the bus voltage back to its desired voltage level. If bus voltage increases, the SVC will inject less (or TCR will absorb more) reactive power (within its control limits), and the result will be to achieve the desired bus voltage. $+Q_{cap}$ is a fixed value, therefore the magnitudes of reactive power injected into the system; Q_{net} is controlled by the magnitude of $-Q_{ind}$ reactive power absorbed by the TCR. Static var systems are applied by utilities in transmission applications for several purposes. The primary purpose is usually rapid control of voltage weak points in a network. Installations may be the midpoint of transmission interconnections or in load areas.

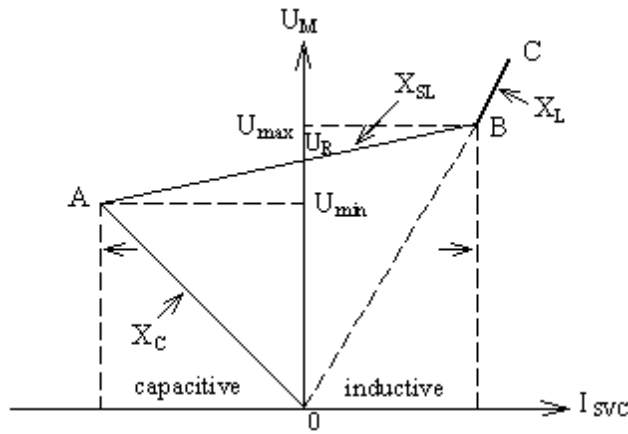


Figure 3.2: SVC V-I characteristic

The SVC can be operated in two different modes: In voltage regulation mode and in var control mode (the SVC susceptance is kept constant) when the SVC is operated in voltage regulation mode, it implements the power system V-I characteristic. As long as the SVC susceptance B stays within the maximum and minimum susceptance values imposed by the total reactive power of capacitor banks (B_{cmax}) at point A and reactor banks (B_{lmax}) at point B, the voltage is regulated at the reference voltage U_R . However, a voltage droop is normally used (usually between 1% and 4% at maximum reactive power output), and the V-I characteristic has the slope. SVC is in regulation range ($-B_{max} < B < B_{Lmax}$).

3.1.3: Midpoint Voltage Regulation for line segmentation

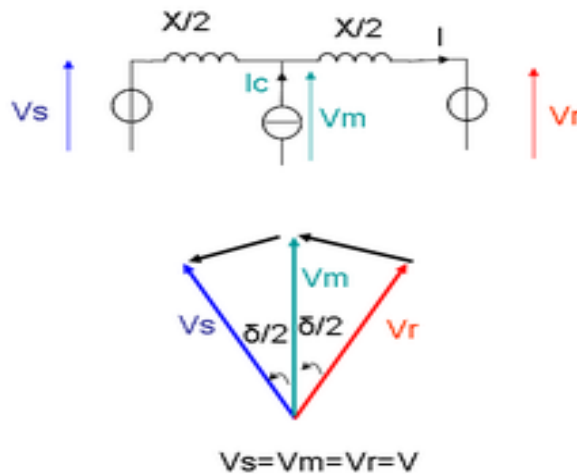


Figure 3.3: Voltage regulation circuit and phasor diagram

It is a two bus transmission model in which an ideal Var compensator is shunt connected at the midpoint of transmission line, as shown in figure 1. For simplicity line is represented by series line inductance. The compensator is represented by sinusoidal ac voltage source (of fundamental frequency), in-phase with the midpoint voltage, V_m and with amplitude identical to that of the sending end and receiving end voltage ($V_m = V_r = V_s = V$). The midpoint compensator in effect segments the transmission line into two independent parts: the first segment, with impedance of $X/2$, carries power from sending end to the midpoint, and second segment, also with an impedance of $X/2$, carries power from the midpoint to receiving end. Corresponding phasor diagram is also shown in fig 1 above.

For the lossless system assume, the real power is the same at each terminal of the line, it can be derived from phasor diagram in fig 1. The transmitted power is found to be double in its magnitude at the expense of a rapidly increasing reactive power demand on the midpoint compensator. It is also evident that the midpoint of the transmission line is the best location for the compensator. This is because the voltage sag along the uncompensated transmission line is the largest at the midpoint. Also, the compensation at the midpoint breaks the transmission line into two equal segments for each of which the maximum transmittable power is same. For unequal segments, the transmittable power of the longer segment would clearly determine the overall transmission limit.

3.2: STATCOM

It is defined by IEEE as “A static synchronous generator operated as a shunt connected static var compensator whose capacitive or inductive output current can be controlled independent of the ac system voltage.”

The static synchronous compensator (STATCOM) is one of the recently developed converter-based flexible AC transmission systems (FACTS) controllers. Usually the reactive output of a STATCOM is regulated to maintain the desired AC voltage at the bus, to which a STATCOM is connected. It is based on a voltage sourced or current sourced converter, from an overall cost point of view, the voltage-sourced converters seem to be preferred. For the voltage sourced converter, its ac output voltage is controlled such that it is just right for the required reactive current flow for any ac bus voltage. Dc capacitor voltage is automatically adjusted as required to serve as a voltage source for the converter.

Similarly to the SVC the STATCOM can provide instantaneous and continuously variable reactive power in response to grid voltage transients, enhancing the grid voltage stability. The STATCOM operates according to voltage source principles, which together with unique PWM (Pulse Width Modulation) switching of IGBTs (Insulated Gate Bipolar Transistors) gives it unequalled performance in terms of effective rating and response speed. The STATCOM provides additional versatility in terms of power quality improvement capabilities.

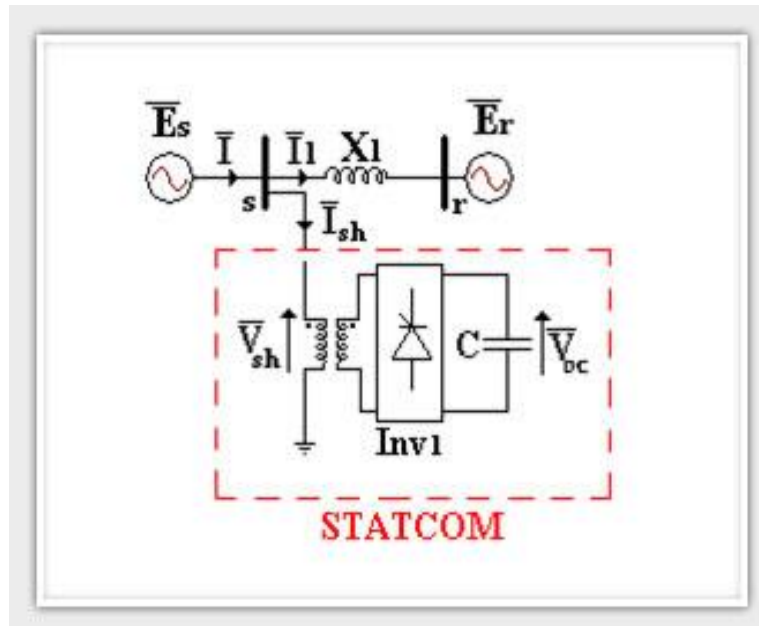


Figure 3.4: STATCOM connection diagram

3.3: SSSC (static synchronous series compensator)

It is defined by IEEE as “A static synchronous generator operated without an external electric energy source as a series compensator whose output voltage is in quadrature with, and controllable independently of, the line current for the purpose of increasing or decreasing the overall reactive voltage drop across the line and thereby controlling the transmitted electric power. The SSSC may include transiently rated energy storage or energy absorbing device to enhance the dynamic behavior of the power system by additional temporary real power compensation, to increase or decrease momentarily, the overall real(resistive) voltage drop across the line.”

It is like STATCOM, except that the output ac voltage is in series with the line. It is based on a voltage sourced or current sourced converter. Usually the injected voltage in series would be quite small compared to the line voltage, and the insulation to ground would be quite high. Without an extra energy source, SSSC can only inject a variable voltage, which is 90 degree leading or lagging the current. The primary of transformer and hence secondary as well as the converter has to carry full line current including the fault current unless the converter is temporarily bypassed during severe line fault

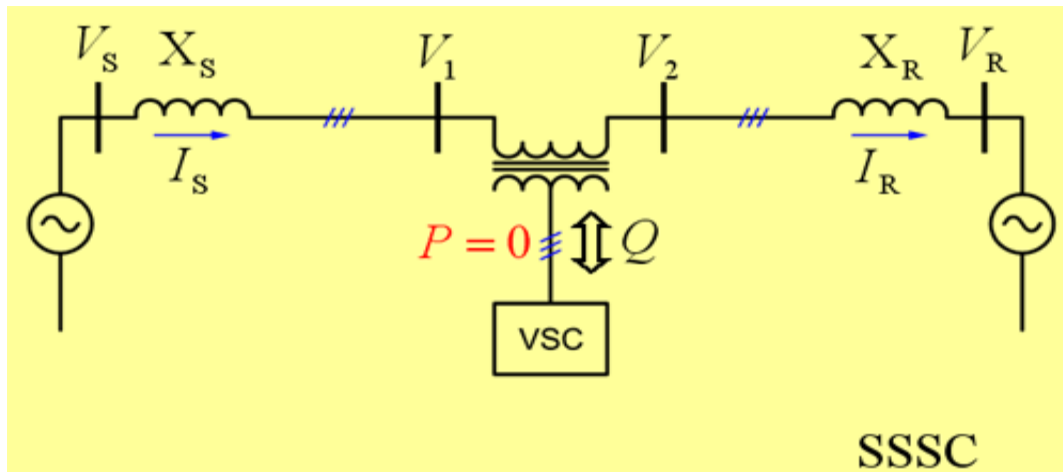


Figure 3.5: SSSC (static synchronous series compensator) connection diagram

3.4: TCSC (Thyristor controlled series capacitor)

It is defined by IEEE as “A capacitive reactance compensator which consists of a series capacitor bank shunted by a thyristor-controlled reactor in order to provide a smoothly variable series capacitive reactance.”

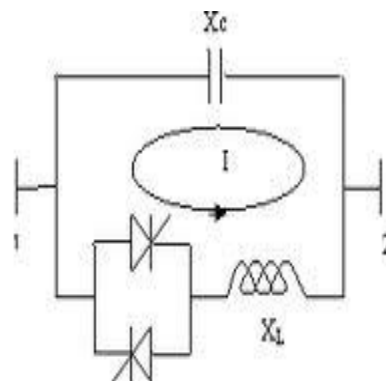


Figure 3.6: TCSC (Thyristor controlled series capacitor) connection diagram

The TCSC is based on thyristors without the gate turn-off capability. It is an alternative to SSSC. A variable reactor such as thyristor controlled reactor (TCR) is connected across a series capacitor. When the TCR firing angle is 180 degrees, the reactor becomes nonconducting and the series capacitor has its normal impedance. As firing angle is advanced from 180 degree to less than 180 degree, the capacitive impedance increases.

At the other end, when the firing angle is 90 degree, the reactor becomes fully conductive, and the total impedance become inductive, because the reactor impedance is designed to be much lower than the series capacitor impedance. With 90 degree firing angle, the TCSC helps in limiting fault current. The TCSC may be a single, large unit, or may consist of several equal or different-sized smaller capacitors in order to achieve superior performances.

3.5: UPFC (Unified power flow controller)

It is defined by IEEE as “A combination of static synchronous compensator (STATCOM) and a static series compensator (SSSC) which are coupled via a common dc link, to allow bidirectional flow of real power between the series output terminal of the SSSC and the shunt output terminal of the STATCOM, and are controlled to provide concurrent real and reactive series line compensation without an external electric energy source. The UPFC, by means of angularly unconstrained series voltage injection, is able to control, concurrently or selectively, the transmission line voltage, impedance, and angle or, alternatively, the real and reactive power flow in line. The UPFC may also provide independently controllable shunt reactive compensation.”

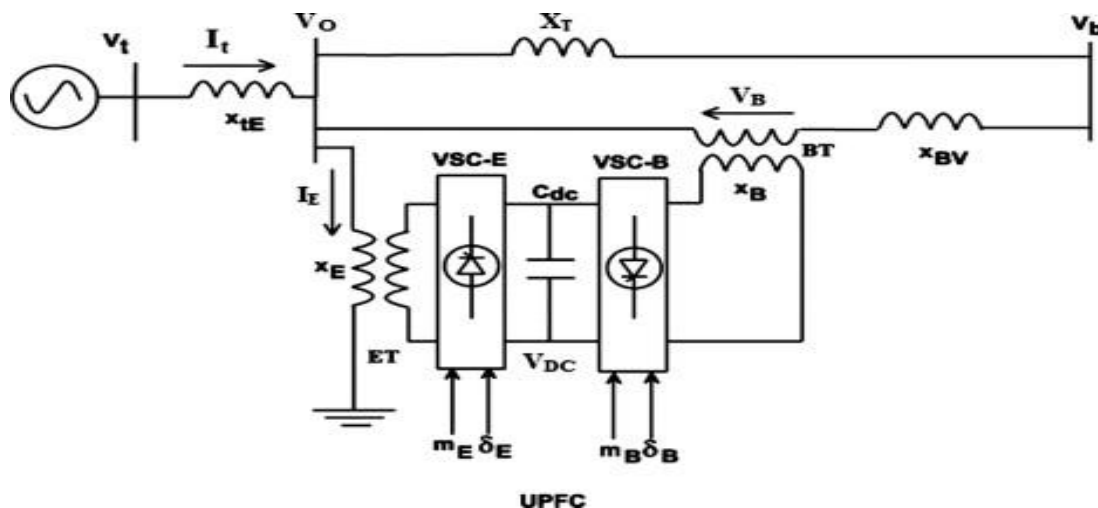


Figure 3.7: UPFC (Unified power flow controller) connection diagram

In UPFC, the active power for the series unit (SSSC) is obtained from the line itself via the shunt unit STATCOM; the latter is also used for voltage control with control of its reactive power. This is a complete controller for controlling active and reactive power control through the line, as well as line voltage control. Additional storage such as superconducting magnet connected to the dc link via an electronic interface would provide the means of further enhancing the effectiveness of the UPFC.

3.6: Benefits from Facts technology

1. Control of power flow as ordered.
2. Increasing loading capability of lines to their thermal capabilities, including short term and seasonal. This can be accomplished by overcoming other limitations, and sharing of power among lines according to their capability. The thermal capability of a line varies by a very large margin based on the environmental conditions and loading history.
3. Increase the system security through raising the transient stability limit, limiting short-circuit currents and overloads, managing cascading blackouts and damping electromechanical oscillation of power system and machines.
4. Provide secure tie line connection to neighboring utilities and regions thereby decreasing overall generation reserve requirements on both sides.
5. Provide greater flexibility in siting new generation.
6. Upgrade of lines.
7. Reduce reactive power flows, thus allowing the lines to carry more active power.
8. Reduce loop flows.
9. Increase utilization of lowest cost generation.

CHAPTER 4

FUZZY LOGIC CONTROLLER

4.1: Introduction

Most of the controllers for FACTS devices are based on the PI controller. Although the PI controllers are simple and easy to design, their performance deteriorates when the system operating conditions vary widely and large disturbances occur. Unlike the PI controllers, Fuzzy Logic Controllers (FLC) is capable of tolerating uncertainty and imprecision to a greater extent so, they produce good results under changing operating conditions and uncertainties in system parameters. Recently fuzzy logic as a novel robust control design method has shown promising results. The emphasis in fuzzy control design center is around uncertainties in the system parameters and operating conditions

Fuzzy control theory is applied to modulate the input signal for static Var compensator to enhance power system stability. The characteristics of power system is non-linear in nature and techniques adopted for damping oscillations that are optimum for one set of operating conditions may not be optimum for another set when conventional control is used. Whatever may be the technique adopted, Fuzzy Logic based controller is likely to be an ideal choice for power system damping because of its adaptable nature. It is possible to design fuzzy logic controller by taking into account the non linearity of power system. It can be implemented easily because complicated and time consuming calculations are not involved.

Fuzzy control system is rule based system in which a set of fuzzy rules represent a control design mechanism. The basic configuration of fuzzy logic controller consists of a fuzzification interface, a knowledge base, decision making logic, and a defuzzification interface. The fuzzy controller used in power system stabilizer is normally a two-input and a single output component. It is usually a MISO system. The fuzzy logic controller (FLC) design consists of following steps.

- 1) Identification of input and output variables.
- 2) Construction of control rules.
- 3) Establishing fuzzification method and fuzzy membership functions.
- 4) Selection of compositional rule of inference.
- 5) Defuzzification method i.e transformation of fuzzy control statement into specific control actions. For this we will use centre of gravity defuzzification procedure.

Features of fuzzy logic –

1. Fuzzy logic can model nonlinear functions of arbitrary complexity.
2. Fuzzy logic can be blended with conventional control techniques.
3. It can be built on top of the experience of experts.
4. It is flexible.

5. It is conceptually easy to understand.
6. It is tolerant of imprecise data.

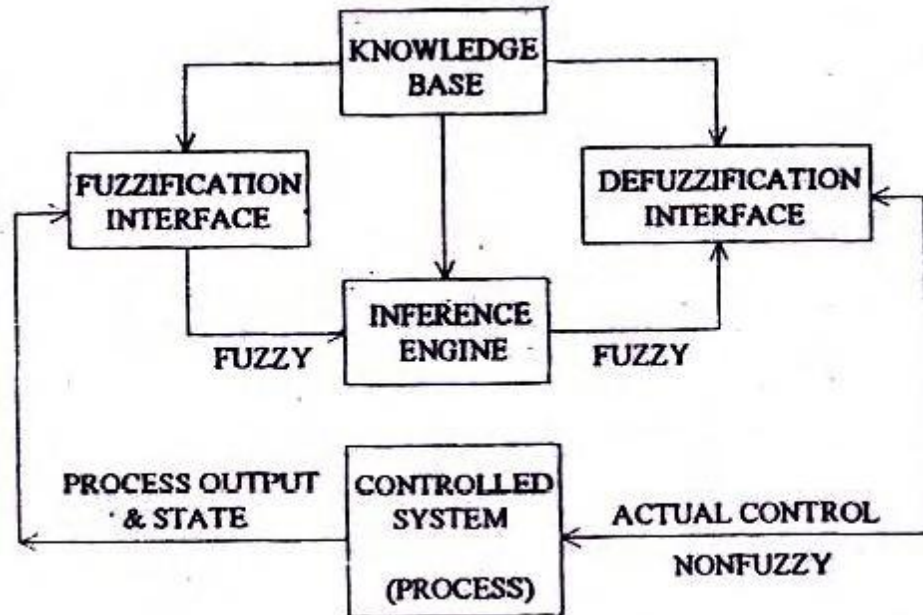


Figure 4.1: General Structure of a Fuzzy Logic System

4.2: Fuzzy inference system

Fuzzy inference is the process of formulating the mapping from a given input to an output using fuzzy logic. The mapping then provides a basis from which decisions can be made, or patterns discerned. The process of fuzzy inference involves all of the pieces that are described in the previous sections: Membership Functions, Logical Operations, and If-Then Rules. You can implement two types of fuzzy inference systems in the toolbox: Mamdani-type and Sugeno-type. These two types of inference systems vary somewhat in the way outputs are determined. See the Bibliography for references to descriptions of these two types of fuzzy inference systems.

Fuzzy inference systems have been successfully applied in fields such as automatic control, data classification, decision analysis, expert systems, and computer vision. Because of its multidisciplinary nature, fuzzy inference systems are associated with a number of names, such as fuzzy-rule-based systems, fuzzy expert systems, fuzzy modeling, fuzzy associative memory, fuzzy logic controllers, and simply (and ambiguously) fuzzy systems.

Mamdani's fuzzy inference method is the most commonly seen fuzzy methodology. Mamdani's method was among the first control systems built using fuzzy set theory. It was proposed in 1975

by Ebrahim Mamdani as an attempt to control a steam engine and boiler combination by synthesizing a set of linguistic control rules obtained from experienced human operators. Mamdani's effort was based on Lotfi Zadeh's 1973 paper on fuzzy algorithms for complex systems and decision processes. Although the inference process described in the next few sections differs somewhat from the methods described in the original paper, the basic idea is much the same.

Mamdani-type inference, as defined for the toolbox, expects the output membership functions to be fuzzy sets. After the aggregation process, there is a fuzzy set for each output variable that needs defuzzification. It is possible, and in many cases much more efficient, to use a single spike as the output membership functions rather than a distributed fuzzy set. This type of output is sometimes known as a singleton output membership function, and it can be thought of as a pre-defuzzified fuzzy set. It enhances the efficiency of the defuzzification process because it greatly simplifies the computation required by the more general Mamdani method, which finds the centroid of a two-dimensional function. Rather than integrating across the two-dimensional function to find the centroid, you use the weighted average of a few data points. Sugeno-type systems support this type of model. In general, Sugeno-type systems can be used to model any inference system in which the output membership functions are either linear or constant.

This section describes the fuzzy inference process and uses the example of the two-input, one-output, three-rule tipping problem The Basic Tipping Problem that you saw in the introduction in more detail. The basic structure of this example is shown in the following diagram:

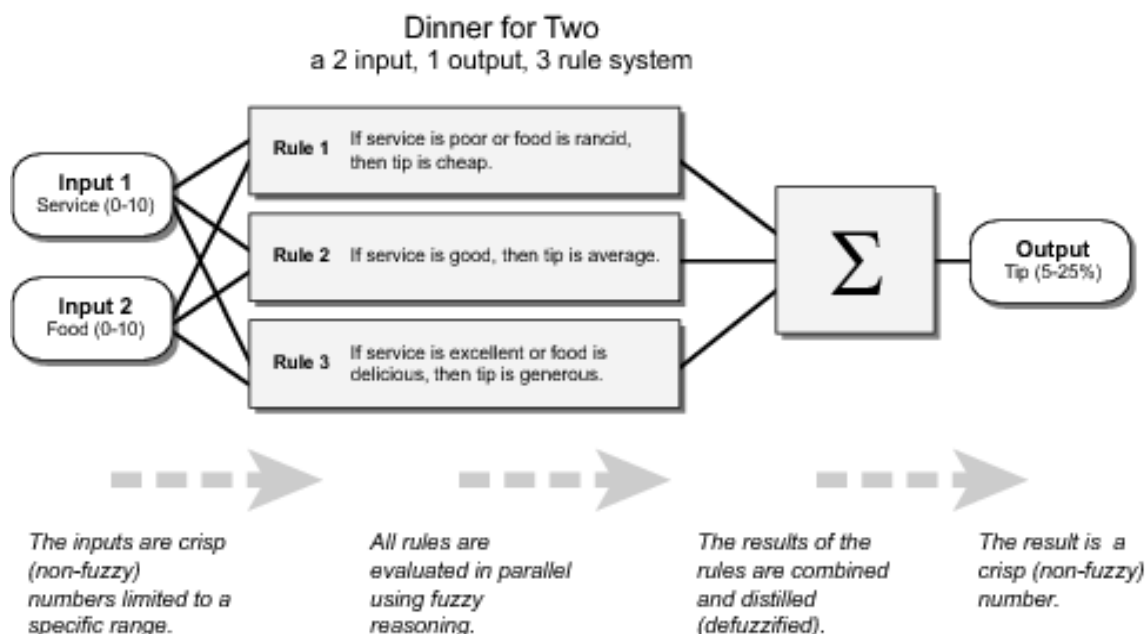


Figure 4.2: Fuzzy inference system

Information flows from left to right, from two inputs to a single output. The parallel nature of the rules is one of the more important aspects of fuzzy logic systems. Instead of sharp switching between modes based on breakpoints, logic flows smoothly from regions where the system's behavior is dominated by either one rule or another.

Fuzzy inference process comprises of five parts: fuzzification of the input variables, application of the fuzzy operator (AND or OR) in the antecedent, implication from the antecedent to the consequent, aggregation of the consequents across the rules, and defuzzification. These sometimes cryptic and odd names have very specific meaning that is defined in the following steps.

4.3: Step 1 Fuzzify inputs

The first step is to take the inputs and determine the degree to which they belong to each of the appropriate fuzzy sets via membership functions. In Fuzzy Logic Toolbox software, the input is always a crisp numerical value limited to the universe of discourse of the input variable (in this case the interval between 0 and 10) and the output is a fuzzy degree of membership in the qualifying linguistic set (always the interval between 0 and 1). Fuzzification of the input amounts to either a table lookup or a function evaluation.

This example is built on three rules, and each of the rules depends on resolving the inputs into a number of different fuzzy linguistic sets: service is poor, service is good, food is rancid, and food is delicious, and so on. Before the rules can be evaluated, the inputs must be fuzzified according to each of these linguistic sets. For example, to what extent is the food really delicious? The following figure shows how well the food at the hypothetical restaurant (rated on a scale of 0 to 10) qualifies, (via its membership function), as the linguistic variable delicious. In this case, we rated the food as an 8, which, given your graphical definition of delicious, corresponds to $\mu = 0.7$ for the delicious membership function.

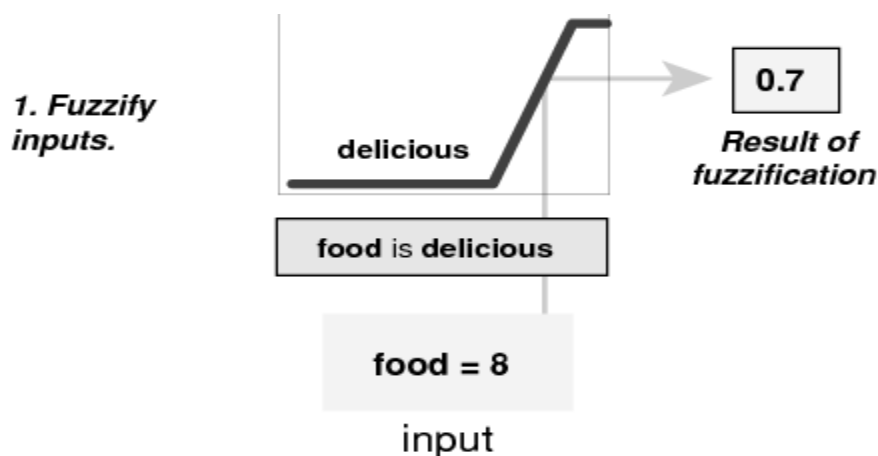


Figure 4.3: Fuzzify inputs

In this manner, each input is fuzzified over all the qualifying membership functions required by the rules.

4.4: Step 2 Apply Fuzzy operator

After the inputs are fuzzified, you know the degree to which each part of the antecedent is satisfied for each rule. If the antecedent of a given rule has more than one part, the fuzzy operator is applied to obtain one number that represents the result of the antecedent for that rule. This number is then applied to the output function. The input to the fuzzy operator is two or more membership values from fuzzified input variables. The output is a single truth value.

As is described in Logical Operations section, any number of well-defined methods can fill in for the AND operation or the OR operation. In the toolbox, two built-in AND methods are supported: min (minimum) and prod (product). Two built-in OR methods are also supported: max (maximum), and the probabilistic OR method *Probor*. The probabilistic OR method (also known as the algebraic sum) is calculated according to the equation

$$Probor(a, b) = a + b - ab$$

In addition to these built-in methods, you can create your own methods for AND and OR by writing any function and setting that to be your method of choice.

The following figure shows the OR operator max at work, evaluating the antecedent of the rule 3 for the tipping calculation. The two different pieces of the antecedent (service is excellent and food is delicious) yielded the fuzzy membership values 0.0 and 0.7 respectively. The fuzzy OR operator simply selects the maximum of the two values, 0.7, and the fuzzy operation for rule 3 is complete. The probabilistic OR method would still result in 0.7.

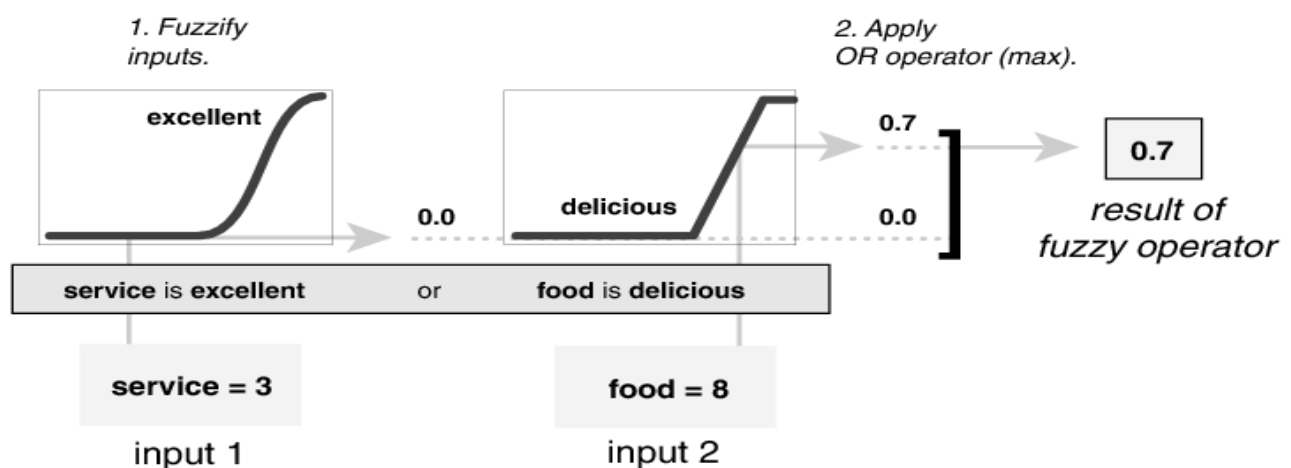


Figure 4.4: Fuzzy operator

4.5: Step 3 Apply implication method

Before applying the implication method, you must determine the rule's weight. Every rule has a weight (a number between 0 and 1), which is applied to the number given by the antecedent. Generally, this weight is 1 (as it is for this example) and thus has no effect at all on the implication process. From time to time you may want to weight one rule relative to the others by changing its weight value to something other than 1.

After proper weighting has been assigned to each rule, the implication method is implemented. A consequent is a fuzzy set represented by a membership function, which weights appropriately the linguistic characteristics that are attributed to it. The consequent is reshaped using a function associated with the antecedent (a single number). The input for the implication process is a single number given by the antecedent, and the output is a fuzzy set. Implication is implemented for each rule. Two built-in methods are supported, and they are the same functions that are used by the AND method: min (minimum), which truncates the output fuzzy, set, and prod (product), which scales the output fuzzy set.

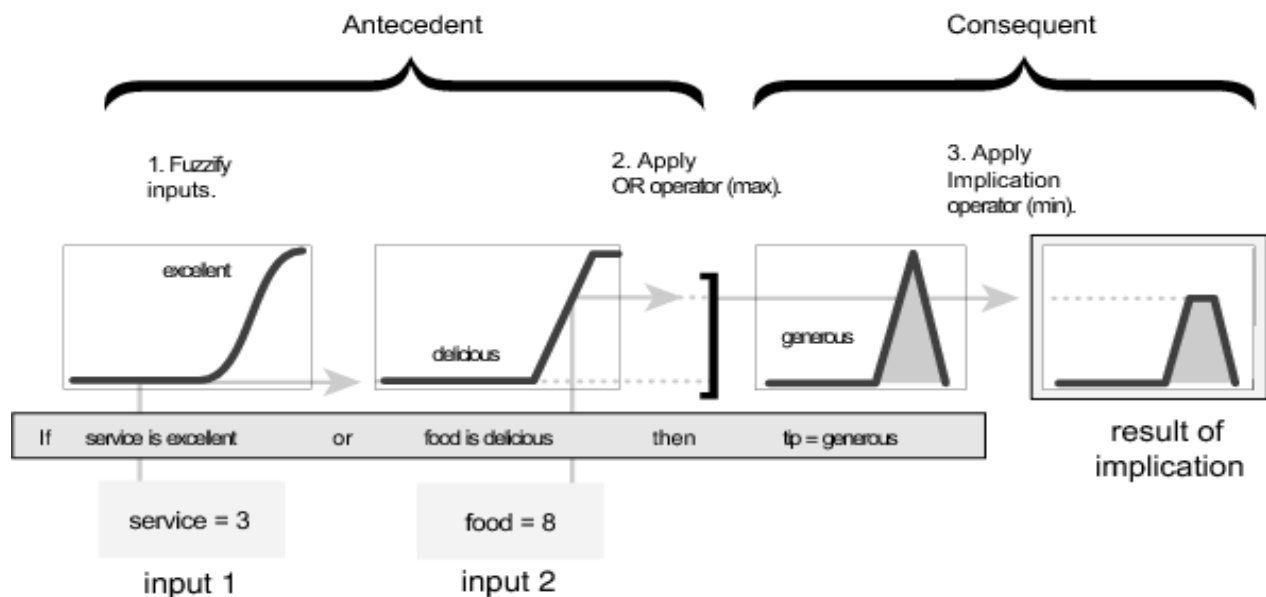


Figure 4.5: Fuzzy implication

4.6: Step 4 Aggregate all outputs

Because decisions are based on the testing of all of the rules in a FIS, the rules must be combined in some manner in order to make a decision. Aggregation is the process by which the fuzzy sets that represent the outputs of each rule are combined into a single fuzzy set. Aggregation only occurs once for each output variable, just prior to the fifth and final step, defuzzification. The input of the aggregation process is the list of truncated output functions returned by the

implication process for each rule. The output of the aggregation process is one fuzzy set for each output variable.

As long as the aggregation method is commutative (which it always should be), then the order in which the rules are executed is unimportant. Three built-in methods are supported:

- max (maximum)
- probor (probabilistic OR)
- sum (simply the sum of each rule's output set)

In the following diagram, all three rules have been placed together to show how the output of each rule is combined, or aggregated, into a single fuzzy set whose membership function assigns a weighting for every output (tip) value.

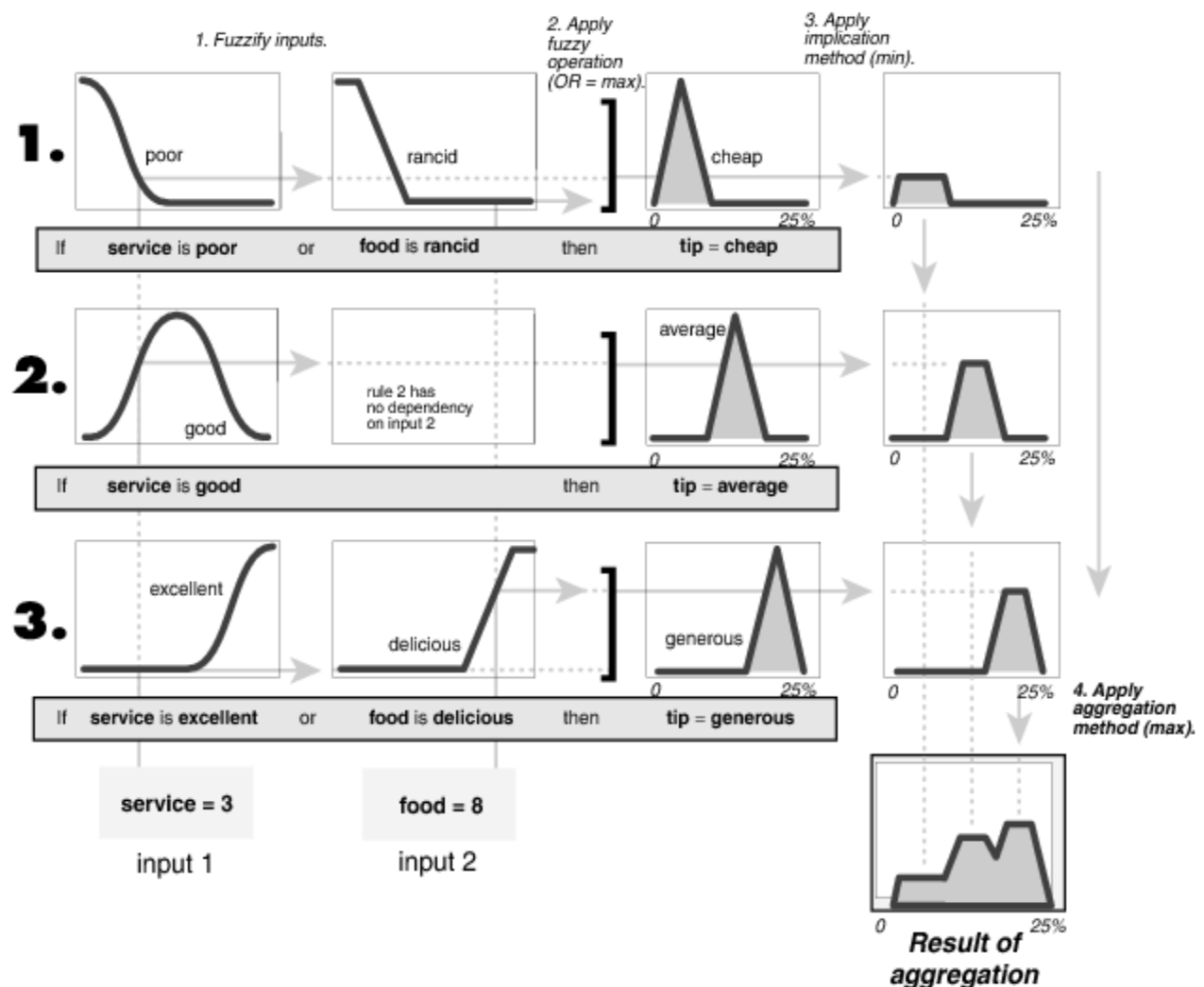


Figure 4.6: Fuzzy aggregate outputs

4.7: Step 5 Defuzzify

The input for the defuzzification process is a fuzzy set (the aggregate output fuzzy set) and the output is a single number. As much as fuzziness helps the rule evaluation during the intermediate steps, the final desired output for each variable is generally a single number. However, the aggregate of a fuzzy set encompasses a range of output values, and so must be defuzzified in order to resolve a single output value from the set.

Perhaps the most popular defuzzification method is the centroid calculation, which returns the center of area under the curve. There are five built-in methods supported: centroid, bisector, middle of maximum (the average of the maximum value of the output set), largest of maximum, and smallest of maximum.

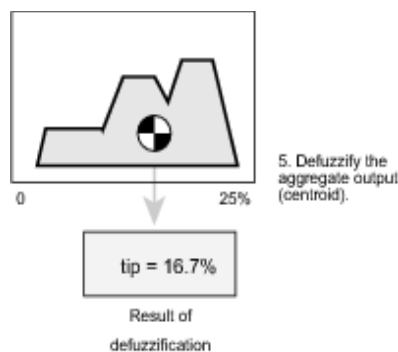


Figure 4.7: Defuzzification

THE FUZZY INFERENCE DIAGRAM

The fuzzy inference diagram is the composite of all the smaller diagrams presented so far in this section. It simultaneously displays all parts of the fuzzy inference process you have examined. Information flows through the fuzzy inference diagram as shown in the following figure.

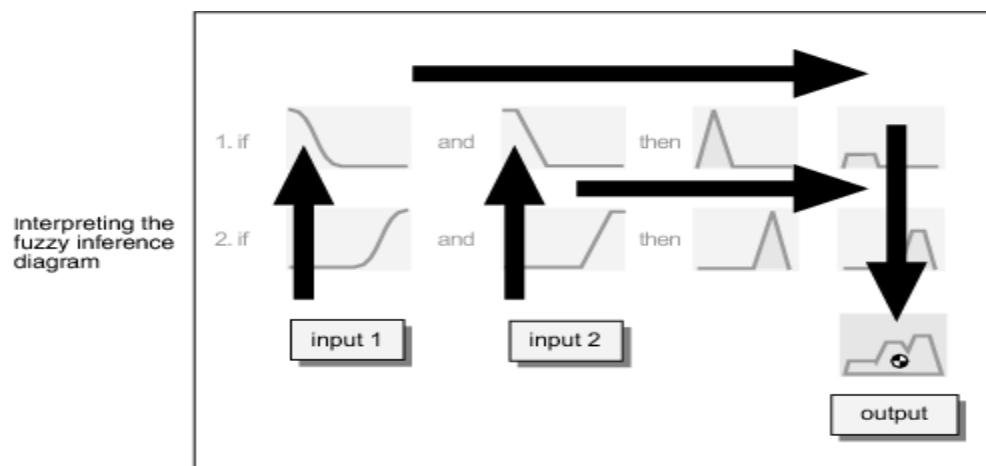
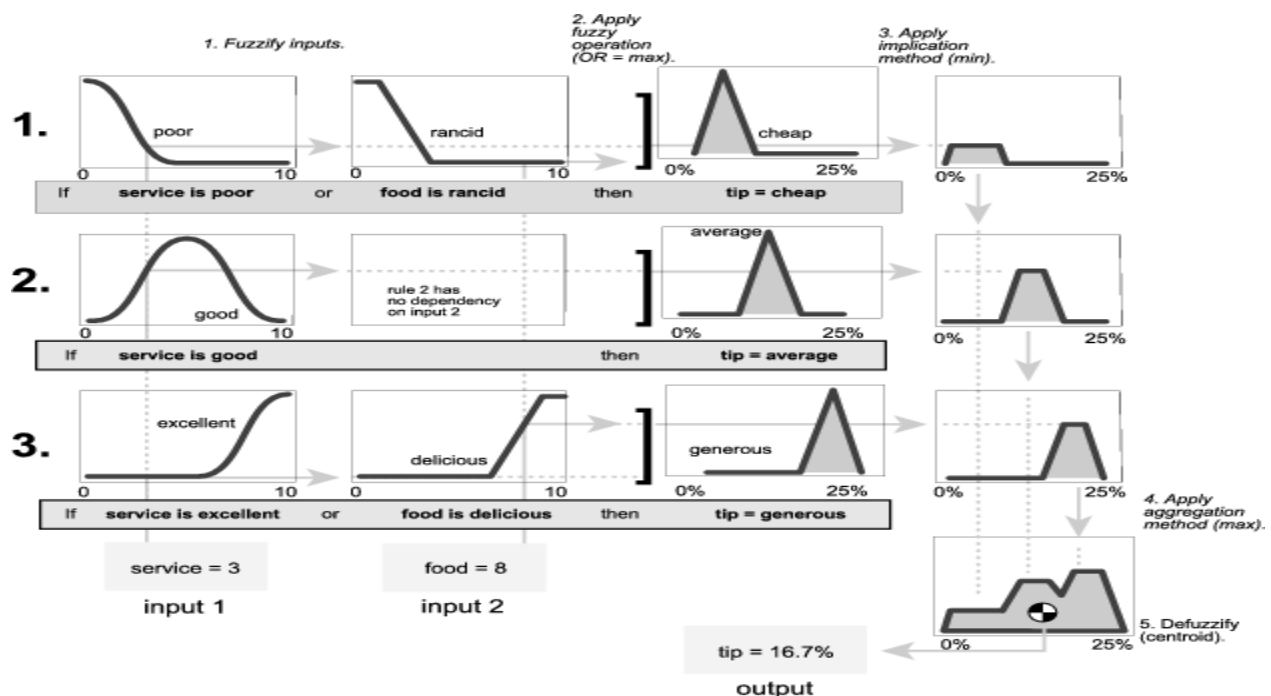


Figure 4.8: Fuzzy inference diagram

In this figure, the flow proceeds up from the inputs in the lower left, then across each row, or rule, and then down the rule outputs to finish in the lower right. This compact flow shows everything at once, from linguistic variable fuzzification all the way through defuzzification of the aggregate output.

The following figure shows the actual full-size fuzzy inference diagram. There is a lot to see in a fuzzy inference diagram, but after you become accustomed to it, you can learn a lot about a system very quickly. For instance, from this diagram with these particular inputs, you can easily see that the implication method is truncation with the min function. The max function is being used for the fuzzy OR operation. Rule 3 (the bottom-most row in the diagram shown previously) is having the strongest influence on the output and so on. The Rule Viewer described in The Rule Viewer is a MATLAB implementation of the fuzzy inference diagram.



4.8: Customization

One of the primary goals of Fuzzy Logic Toolbox software is to have an open and easily modified fuzzy inference system structure. The toolbox is designed to give you as much freedom as possible, within the basic constraints of the process described, to customize the fuzzy inference process for your application.

Building Systems with Fuzzy Logic Toolbox Software describes exactly how to build and implement a fuzzy inference system using the tools provided. To learn how to customize a fuzzy inference system, see Building Fuzzy Inference Systems Using Custom Functions.

Fuzzy control appears to be the most suitable one, due to its robustness and lower computation burden. The fuzzy logic controllers could easily be constructed using a simple micro-computer. The supplementary stabilizing signal is determined using fuzzy membership.

CHAPTER 5

CASE STUDY AND RESULTS

5.1: State space modelling of svc controller with rotor speed Deviation as supplementary signal and simulation result.

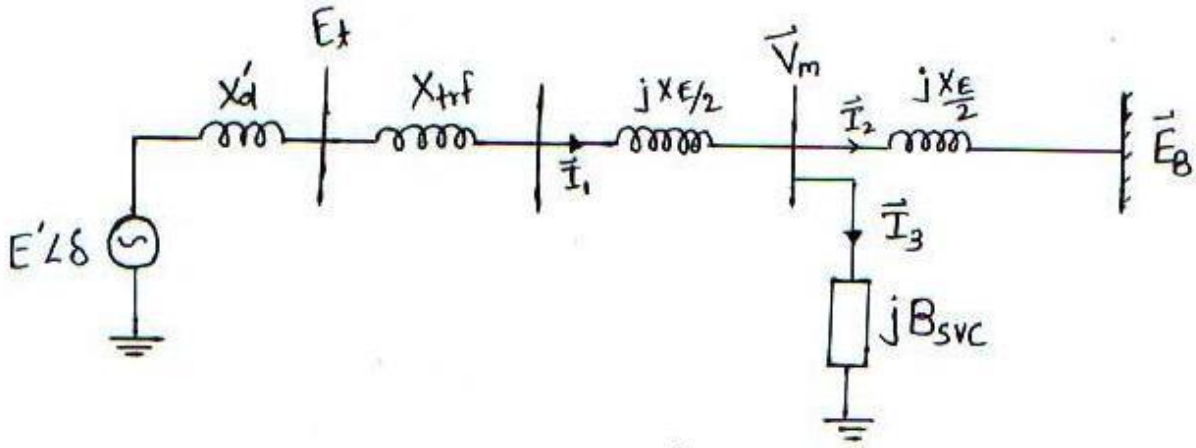


Figure 5.1: SMIB system with SVC

From fig 5.1,

$$X_t = X_d' + X_{trf} + \frac{X_E}{2}$$

$$\Rightarrow \vec{I}_1 = \vec{I}_2 + \vec{I}_3$$

$$\Rightarrow \frac{\vec{E}' - \vec{V}_m}{jX_t} = \frac{\vec{V}_m - \vec{E}_B}{0.5jX_E} + \vec{V}_m * jB_{SVC}$$

$$\vec{V}_m * \left(jB_{SVC} - \frac{j2}{X_E} - \frac{j}{X_t} \right) = \frac{E' * \cos\delta + E' * j\sin\delta}{jX_t} + \frac{2E_B}{jX_E}$$

$$\Rightarrow \vec{V}_m = \frac{E'X_E\cos\delta + 2E_BX_t}{X_E + 2X_t - X_EX_tB_{SVC}} + j * \frac{E'X_E\sin\delta}{X_E + 2X_t - X_EX_tB_{SVC}}$$

$$\text{let } X = X_E + 2X_t - X_EX_tB_{SVC}$$

$$V_m = \left[\frac{\left\{ (E'X_E \cos \delta + 2X_t E_B)^2 + (E'X_E \sin \delta)^2 \right\}}{\{X\}^2} \right]^{\frac{1}{2}}$$

$$\Rightarrow V_m = f(\delta, B_{SVC})$$

$$\Delta V_m = \left(\frac{\partial V_m}{\partial \delta} \right) * \Delta \delta + \left(\frac{\partial V_m}{\partial B_{SVC}} \right) * \Delta B_{SVC}$$

$$\Delta V_m = - \left[\left\{ \frac{2E'E_B X_E X_t \sin \delta}{V_m * X * X} \right\} \Delta \delta + \left\{ \frac{-V_m X_t X_E}{X} \right\} \Delta B_{SVC} \right] = -[c1 \Delta \delta + c2 \Delta B_{SVC}] \quad \dots \dots (a)$$

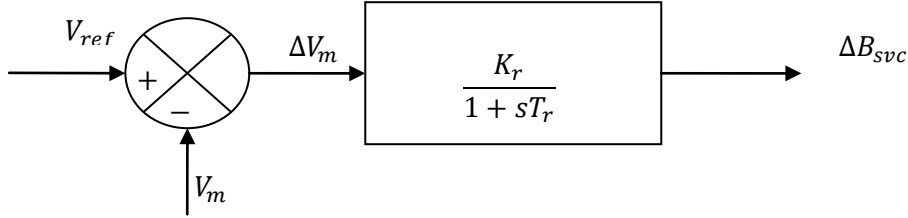


Figure 5.2: Block diagram of SVC voltage regulator

From fig 5.2,

$$SVC \text{ CONTROLLER} \Rightarrow \Delta B_{SVC} = \frac{K_r}{1 + sT_r} \Delta V_m \quad \dots \dots (b)$$

$$\Delta B_{SVC} (1 + sT_r) = -K_r (c1 \Delta \delta + c2 \Delta B_{SVC})$$

$$\Delta B_{SVC} \cdot = \left(\frac{-K_r * c1}{T_r} \right) \Delta \delta - \left(\frac{(1 + K_r * c2)}{T_r} \right) \Delta B_{SVC} \quad \dots \dots (1)$$

ΔTe calculation

$$\vec{I}_2 = \frac{\vec{V}_m - \vec{E}_B}{\frac{jX_E}{2}} = -\frac{j2}{X_E} \left[\frac{\{(E'X_E \cos \delta + 2E_B X_t) + (jE'X_E \sin \delta)\}}{X} - E_B \right]$$

$$\overline{(I_2^*)} = \frac{2}{X * X_E} [(E' X_E \sin \delta) + j * (E' X_E \cos \delta + 2E_B X_t - X E_B)]$$

$$\text{in p.u,} \quad Pe = Te = \text{real} [E_B * \overline{(I_2^*)}] = E_B * \left[\frac{2X_E E' \sin \delta}{X X_E} \right] = \frac{2E' E_B \sin \delta}{X}$$

$$\Delta Te = \left(\frac{\partial Te}{\partial \delta} \right) * \Delta \delta + \left(\frac{\partial Te}{\partial B_{SVC}} \right) * \Delta B_{SVC}$$

$$\frac{2E' E_B \cos \delta}{X} \Delta \delta + \frac{-2E' E_B \sin \delta}{X * X} * (-X_t X_E) \Delta B_{SVC}$$

$$\Delta Te = \left[\frac{2E' E_B \cos \delta}{X} \right] \Delta \delta + \left[\frac{2E' E_B X_t X_E \sin \delta}{X * X} \right] \Delta B_{SVC}$$

$$= c1' \Delta \delta + c2' \Delta B_{SVC} \quad \dots \dots (c)$$

$$\text{where, } c1' = \frac{2E' E_B \cos \delta}{X} \quad \text{and} \quad c2' = \frac{2E' E_B X_t X_E \sin \delta}{X * X}$$

equation of motion with SVC,

$$\dot{\Delta \delta} = w_o * \Delta w_r \quad \dots \dots \dots (2)$$

$$\Delta \dot{w}_r = \frac{\Delta Tm - \Delta Te - K_d \Delta w_r}{2H}$$

$$\Delta \dot{w}_r = \frac{\Delta Tm - (c1' \Delta \delta + c2' \Delta B_{SVC}) - K_d \Delta w_r}{2H} \quad \dots \dots \dots (3)$$

equation 1 & 2 & 3 in vector matrix form,

$$\begin{bmatrix} \Delta \dot{w}_r \\ \Delta \dot{\delta} \\ \Delta \dot{B}_{SVC} \end{bmatrix} = \begin{bmatrix} \frac{-K_d}{2H} & \frac{-c1'}{2H} & \frac{-c2'}{2H} \\ w_o & 0 & 0 \\ 0 & \frac{-K_r c1}{T_r} & \frac{1 + K_r c2}{T_r} \end{bmatrix} \begin{bmatrix} \Delta w_r \\ \Delta \delta \\ \Delta B_{SVC} \end{bmatrix} + \begin{bmatrix} \frac{1}{2H} \\ 0 \\ 0 \end{bmatrix} \Delta Tm$$

...State equation with SVC

laplace transfer of equation (3) gives,

$$\Delta \delta = \frac{w_o}{s} * \left[\frac{\{\Delta Tm - (c1' \Delta \delta + c2' \Delta B_{SVC}) - K_d \Delta w_r\}}{\{2Hs\}} \right] \dots \dots (4)$$

As rotor speed is taken as supplementary signal,

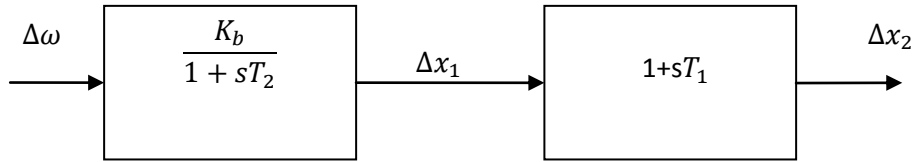


Figure 5.3: Damping controller using rotor speed

From fig 5.3,

$$\Delta x_1 = \Delta w * \frac{K_b}{1 + sT_2}$$

$$\Rightarrow \Delta \dot{x}_1 = \left(-\frac{1}{T_2}\right) \Delta x_1 + \left(\frac{K_b}{T_2}\right) \Delta w \dots \dots (6)$$

$$\& \Delta x_2 = (1 + sT_1) \Delta x_1$$

$$\Delta x_2 = \Delta x_1 \left(1 - \frac{T_1}{T_2}\right) + \left(\frac{T_1 K_b}{T_2}\right) \Delta w$$

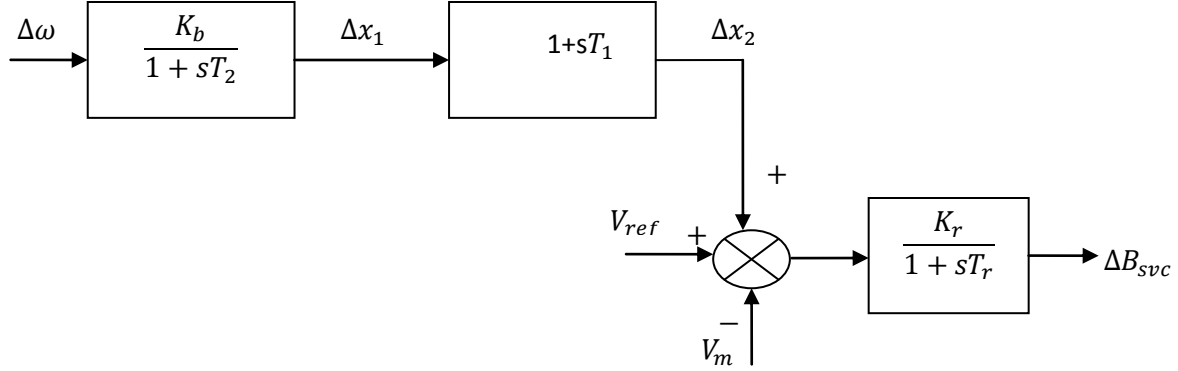


Figure 5.4: Composite block diagram of SVC damping controller (using rotor speed)

From fig 5.4,

$$\Delta B_{svc} = \frac{K_r}{1 + sT_r} \{ \Delta V_m + \Delta x_2 \} \quad \dots \quad (6')$$

$$\Delta B_{svc} = \frac{K_r}{1 + sT_r} \left[-[c_1 \Delta \delta + c_2 \Delta B_{svc}] + \Delta x_1 \left(1 - \frac{T_1}{T_2}\right) + \left(\frac{T_1 K_b}{T_2}\right) \Delta w \right]$$

$$\begin{aligned} (1 + sT_r)(\Delta B_{svc}) \\ = K_r \left(1 - \frac{T_1}{T_2}\right) \Delta w * \frac{K_b}{1 + sT_2} + K_r * \frac{T_1 K_b}{T_2} * \Delta w - K_r (c_1 \Delta \delta + c_2 \Delta B_{svc}) \end{aligned}$$

$$\Delta \dot{B}_{svc} = K_3 \Delta w + K_4 \Delta \delta + K_5 \Delta B_{svc} \quad \dots \quad (7)$$

$$\text{where, } K_3 = \left[\left(1 - \frac{T_1}{T_2}\right) * \frac{K_b}{(1 + sT_2) * T_r} + K_r * \frac{T_1 K_b}{T_2 * T_r} \right] * \Delta w$$

$$\& \quad K_4 = - \left\{ \frac{K_r c_1}{T_r} \right\}$$

$$K5 = -(1 + c2) * Kr * \frac{1}{Tr}$$

$$\Delta B_{SVC} = K6 \Delta w + K7 \Delta \delta \quad \dots \dots (8) \text{ where, } K6 = K3 * \frac{T_r}{(1 + c2) * K_r + s * T_r} \text{ \&}$$

$$K7 = K4 * T_r / ((1 + c2) * K_r + s * T_r)$$

CASE STUDY

Given, $P = 0.9 \text{ p.u}$ & $Q = 0.3 \text{ p.u}$, $X_d' = 0.3 \text{ p.u}$, $X_{trf} = 0.15 \text{ p.u}$, $X_E = 0.5$;

$$I_1 = \left\{ \frac{P + j * Q}{E_t} \right\}^* = 0.9 - j0.3 \text{ p.u}$$

$$E' = E_t + jX_d' I_1 = 1.09 + j0.27 = 1.123 (13.92^\circ)$$

Angle by which E_t leads E_B is 36°

So Angle by which E' leads E_B is $(36^\circ + 13.92^\circ) = (49.92^\circ)$

$$\text{so, } X_t = X_d' + X_{trf} + \frac{X_E}{2} = 0.3 + 0.15 + 0.25 = 0.7 \text{ p.u}$$

$$\& V_m = 0.9507 \text{ p.u}$$

$$\& c1' = 0.757 \text{ p.u} ; c2' = 0.1658 \text{ p.u} ; c1 = 0.1744 \text{ p.u} ; c2 = -0.1751$$

$$Kb = 9.5, Kr = 20, Tr = 0.02, \frac{T1}{T2} = 1$$

$$K1 = 5.94, K2 = -1.28$$

$$\text{So, } K6 = \frac{9.5}{0.02s + 16.498} \quad \& \quad K7 = -\frac{-3.488}{0.02s + 16.498}$$

$K6$ is transfer function 2 and $K7$ is transfer function 3 in given figure 5.7. Value of Gain 1 is kept zero that shows a undamped system.

BLOCKDIAGRAM

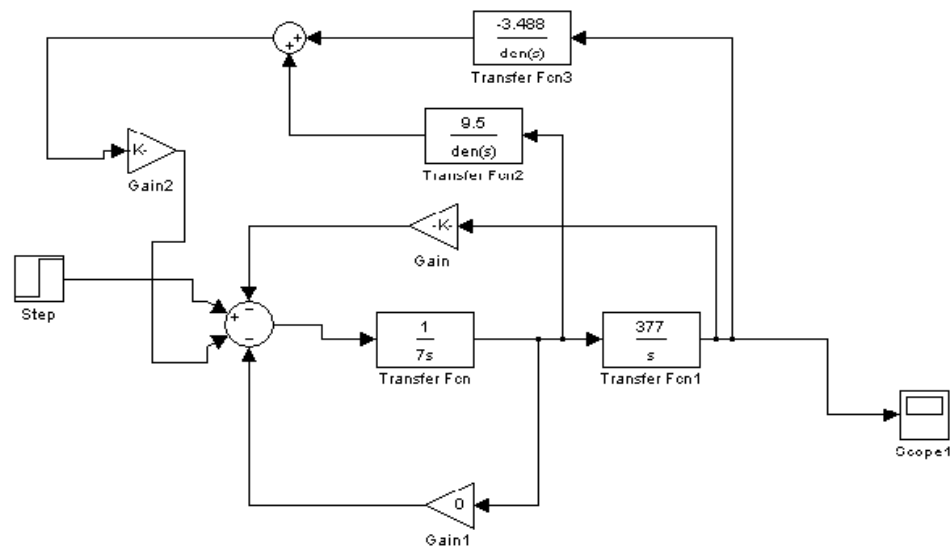


Figure5.7: SIMULINK modelling of SVC damping controller (rotor speed)

SIMULATION RESULT

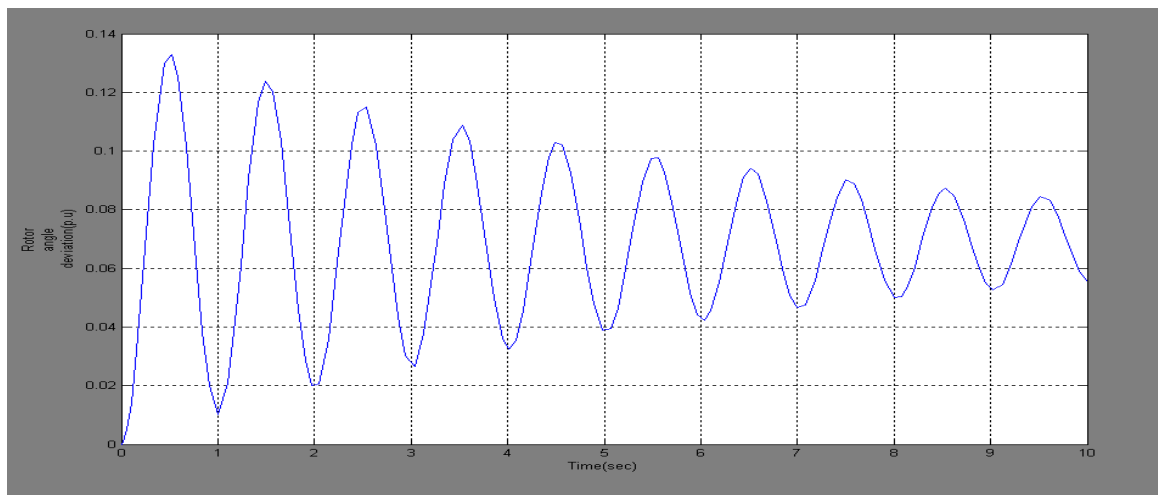


Figure 5.8: Result with rotor speed deviation

State space model of SVC controller using rotor speed as supplementary signal for damping power system oscillation is prepared and their corresponding block diagram is drawn. Simulation result on MATLAB is given in figure below, which shows a damped system, in which SVC based SMIB unstable system is regaining its original equilibrium point with gradually reducing oscillation to zero value of its amplitude. So here system is under damped.

5.2: State space modelling of svc controller with line current Deviation as supplementary signal and simulation result.

From fig 5.1

$$\begin{aligned}
 X_t &= X_d' + X_{trf} + \frac{X_E}{2} \\
 \Rightarrow \quad \vec{I}_1 &= \vec{I}_2 + \vec{I}_3 \\
 \Rightarrow \quad \frac{\vec{E}' - \vec{V}_m}{jX_t} &= \frac{\vec{V}_m - \vec{E}_B}{0.5jX_E} + \vec{V}_m * jB_{SVC} \\
 \vec{V}_m * \left(jB_{SVC} - \frac{j2}{X_E} - \frac{j}{X_t} \right) &= \frac{E' * \cos\delta + E' * j\sin\delta}{jX_t} + \frac{2E_B}{jX_E} \\
 \Rightarrow \vec{V}_m &= \frac{E'X_E\cos\delta + 2E_BX_t}{X_E + 2X_t - X_EX_tB_{SVC}} + j * \frac{E'X_E\sin\delta}{X_E + 2X_t - X_EX_tB_{SVC}}
 \end{aligned}$$

$$\text{let } X = X_E + 2X_t - X_EX_tB_{SVC}$$

$$V_m = \left[\frac{\left\{ \left(E'X_E\cos\delta + 2X_tE_B \right)^2 + \left(E'X_E\sin\delta \right)^2 \right\}^{\frac{1}{2}}}{\{X\}^2} \right]^{\frac{1}{2}}$$

$$\Rightarrow V_m = f(\delta, B_{SVC})$$

$$\Delta V_m = \left(\frac{\partial V_m}{\partial \delta} \right) * \Delta\delta + \left(\frac{\partial V_m}{\partial B_{SVC}} \right) * \Delta B_{SVC}$$

$$\Delta V_m = - \left[\left\{ \frac{2E'E_BX_EX_t\sin\delta}{V_m * X * X} \right\} \Delta\delta + \left\{ \frac{-V_mX_tX_E}{X} \right\} \Delta B_{SVC} \right] = -[c1\Delta\delta + c2\Delta B_{SVC}] \quad \dots \dots (a)$$

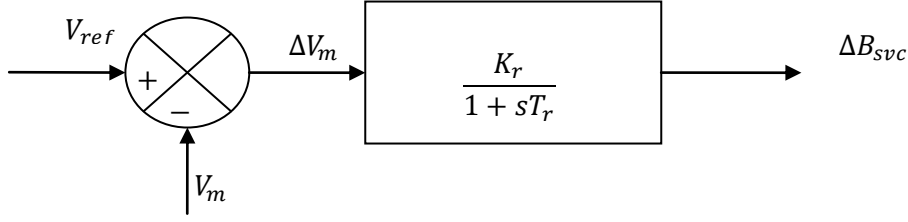


Figure 5.2: Block diagram of SVC voltage regulator

From fig 5.2

$$SVC \text{ CONTROLLER} \Rightarrow \Delta B_{svc} = \frac{K_r}{1 + sT_r} \Delta V_m \quad \dots \dots (b)$$

$$\Delta B_{svc}(1 + sT_r) = -K_r(c_1\Delta\delta + c_2\Delta B_{svc})$$

$$\Delta \dot{B}_{svc} = \left(\frac{-K_r * c_1}{T_r} \right) \Delta\delta - \left(\frac{(1 + K_r * c_2)}{T_r} \right) \Delta B_{svc} \quad \dots \dots (1)$$

ΔT_e calculation

$$\vec{I}_2 = \frac{\vec{V}_m - \vec{E}_B}{\frac{jX_E}{2}} = -\frac{j2}{X_E} \left[\left\{ \frac{(E'X_E \cos\delta + 2E_B X_t) + (jE'X_E \sin\delta)}{X} - E_B \right\} \right]$$

$$\overline{(I_2^*)} = \frac{2}{X * X_E} [(E'X_E \sin\delta) + j * (E'X_E \cos\delta + 2E_B X_t - XE_B)]$$

$$\text{in p.u.,} \quad P_e = T_e = \text{real} [E_B * \overline{(I_2^*)}] = E_B * \left[\frac{2X_E E' \sin\delta}{XX_E} \right] = \frac{2E' E_B \sin\delta}{X}$$

$$\Delta T_e = \left(\frac{\partial T_e}{\partial \delta} \right) * \Delta\delta + \left(\frac{\partial T_e}{\partial B_{svc}} \right) * \Delta B_{svc}$$

$$\frac{2E'E_B \cos \delta}{X} \Delta \delta + \frac{-2E'E_B \sin \delta}{X * X} * (-X_t X_E) \Delta B_{SVC}$$

$$\begin{aligned} \Delta T_e &= \left[\frac{2E'E_B \cos \delta}{X} \right] \Delta \delta + \left[\frac{2E'E_B X_t X_E \sin \delta}{X * X} \right] \Delta B_{SVC} \\ &= c1' \Delta \delta + c2' \Delta B_{SVC} \quad \dots \dots (c) \end{aligned}$$

$$\text{where, } c1' = \frac{2E'E_B \cos \delta}{X} \quad \text{and} \quad c2' = \frac{2E'E_B X_t X_E \sin \delta}{X * X}$$

equation of motion with SVC,

$$\dot{\Delta \delta} = w_o * \Delta w_r \quad \dots \dots \dots (2)$$

$$\Delta \dot{w}_r = \frac{\Delta T_m - \Delta T_e - K_d \Delta w_r}{2H}$$

$$\Delta \dot{w}_r = \frac{\Delta T_m - (c1' \Delta \delta + c2' \Delta B_{SVC}) - K_d \Delta w_r}{2H} \quad \dots \dots \dots (3)$$

equation 1 & 2 & 3 in vector matrix form,

$$\begin{bmatrix} \Delta \dot{w}_r \\ \dot{\Delta \delta} \\ \Delta \dot{B}_{SVC} \end{bmatrix} = \begin{bmatrix} \frac{-K_d}{2H} & \frac{-c1'}{2H} & \frac{-c2'}{2H} \\ w_o & 0 & 0 \\ 0 & \frac{-K_r c1}{T_r} & \frac{1 + K_r c2}{T_r} \end{bmatrix} \begin{bmatrix} \Delta w_r \\ \Delta \delta \\ \Delta B_{SVC} \end{bmatrix} + \begin{bmatrix} \frac{1}{2H} \\ 0 \\ 0 \end{bmatrix} \Delta T_m$$

.... State equation with SVC

laplace transfer of equation (3) gives,

$$\Delta \delta = \frac{w_o}{s} * \left[\frac{\{\Delta T_m - (c1' \Delta \delta + c2' \Delta B_{SVC}) - K_d \Delta w_r\}}{\{2Hs\}} \right] \quad \dots \dots \dots (4)$$

$$As \overrightarrow{I_2} = \frac{\overrightarrow{V_m} - \overrightarrow{E_B}}{\frac{jX_E}{2}} = -\frac{j2}{X_E} \left[\left\{ \frac{(E'X_E \cos \delta + 2E_B X_t) + (jE'X_E \sin \delta)}{X} - E_B \right\} \right]$$

$$I_2 = \{(E'X_E \sin \delta)^2 + (E_B X - E'X_E \cos \delta - 2E_B X_t)^2\} * \left\{ \frac{2}{XX_E} \right\}$$

$$\Delta I_2 = \left\{ \frac{\partial I_2}{\partial \delta} \right\} * \Delta \delta + \left\{ \frac{\partial I_2}{\partial B_{SVC}} \right\} * \Delta B_{SVC}$$

$$\Delta I_2 = \left[(4E'E_B \sin \delta) + \frac{8E_B E' \sin \delta X_t}{X} \right] \Delta \delta + \left[\frac{2E'^2 XX_E^2 X_t}{X^2} - (2X_t * E_B^2) + \frac{8E_B^2 X_t^3}{X^2} - \frac{(8E_B E' X_t^2 X_E \cos \delta)}{X^2} \right] \Delta B_{SVC}$$

$$\Delta I_2 = K1 \Delta \delta + K2 \Delta B_{SVC}$$

As Line current is taken as supplementary control signal,

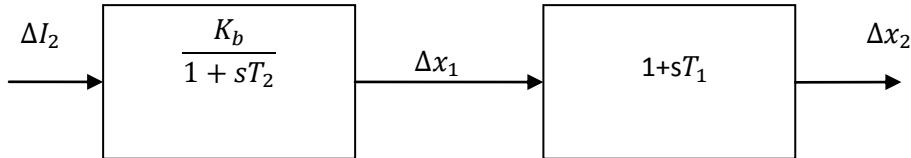


Figure 5.5: Damping controller using line current

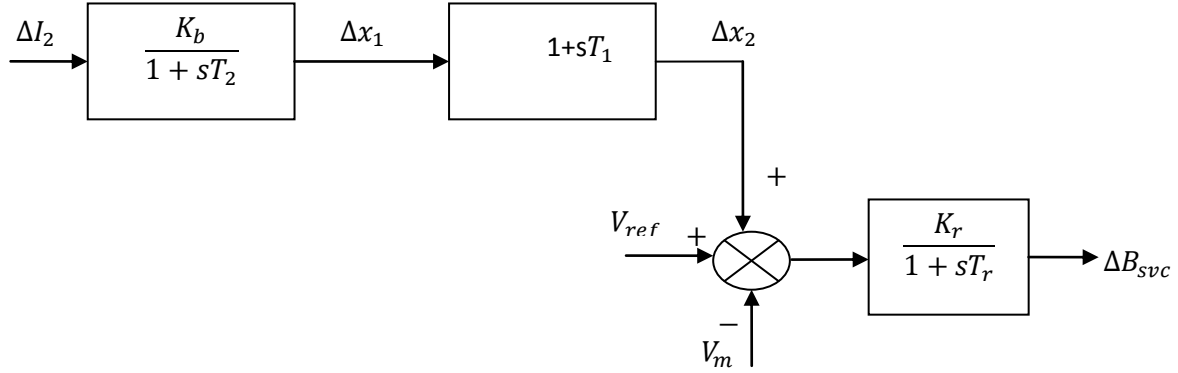


Figure 5.6: Composite block diagram of SVC damping controller (using line current)

From fig 5.5 & 5.6,

$$\Delta x_1 = \Delta I_2 * \frac{K_b}{1 + sT_2}$$

$$\Rightarrow \Delta \dot{x}_1 = \left(-\frac{1}{T_2}\right) \Delta x_1 + \left(\frac{K_b}{T_2}\right) \Delta I_2 \dots \quad \dots (6)$$

$$\& \quad \Delta x_2 = (1 + sT_1) \Delta x_1$$

$$\Delta x_2 = \Delta x_1 \left(1 - \frac{T_1}{T_2}\right) + \left(\frac{T_1 K_b}{T_2}\right) \Delta I_2$$

$$\Delta B_{SVC} = \frac{K_r}{1 + sT_r} \{\Delta V_m + \Delta x_2\} \dots \quad (6')$$

$$\Delta B_{SVC} = \frac{K_r}{1 + sT_r} [-[c1\Delta\delta + c2\Delta B_{SVC}] + \Delta x_1 \left(1 - \frac{T_1}{T_2}\right) + \left(\frac{T_1 K_b}{T_2}\right) \Delta I_2]$$

$$(1 + sT_r)(\Delta B_{SVC})$$

$$= K_r \left(1 - \frac{T_1}{T_2}\right) \Delta x_1 + \frac{T_1 K_b}{T_2} * K_r (K1\Delta\delta + K2\Delta B_{SVC}) - K_r (c1\Delta\delta + c2\Delta B_{SVC})$$

$$\Delta \dot{B}_{SVC} = K3\Delta x_1 + K4\Delta\delta + K5\Delta B_{SVC} \quad (7)$$

$$\text{where, } K3 = \left(\frac{K_r}{T_r}\right) \left(1 - \left(\frac{T_1}{T_2}\right)\right) \&$$

$$K4 = \frac{K_r K_b T_1 K1}{T_2 T_r} - \left\{ \frac{K_r c1}{T_r} \right\}$$

$$K5 = \frac{K_r K_b T_1 K1}{T_2 T_r} - \left\{ \frac{K_r c2}{T_r} \right\} - \frac{1}{T_r}$$

Using equation 2&3 &6&7, state matrix is written as

$$s\Delta B_{SVC} - K5\Delta B_{SVC} = K4\Delta\delta + \frac{K3Kb}{1 + s T_2} \Delta I_2$$

$$\Delta B_{SVC} = K6\Delta\delta + K7 \Delta I_2 \quad (8)$$

$$\text{where, } K6 = \frac{K4}{s - K5} \& \quad K7 = \frac{K3Kb}{(1 + s T_2)(s - K5)}$$

Given, $P = 0.9 \text{ p.u}$ & $Q = 0.3 \text{ p.u}$, $X_d' = 0.3 \text{ p.u}$, $X_{trf} = 0.15 \text{ p.u}$, $X_E = 0.5$;

$$I_1 = \left\{ \frac{P + j * Q}{E_t} \right\}^* = 0.9 - j0.3 \text{ p.u}$$

$$E' = E_t + jX_d' I_1 = 1.09 + j0.27 = 1.123 (13.92^\circ)$$

Angle by which E_t leads E_B is 36°

So Angle by which E' leads E_B is $(36^\circ + 13.92^\circ) = (49.92^\circ)$

$$\text{so, } X_t = X_d' + X_{trf} + \frac{X_E}{2} = 0.3 + 0.15 + 0.25 = 0.7 \text{ p.u}$$

$$\& V_m = 0.9507 \text{ p.u}$$

$$\& c1' = 0.757 p.u ; c2' = 0.1658 p.u ; c1 = 0.1744 p.u ; c2 = -0.1751$$

$$Kb = 9.5, Kr = 20,$$

$$, T1 = 0.2, T2 = 0.02$$

$$K1 = 5.94, K2 = -1.28$$

$$So, K6 = \frac{564296.51}{s + 121569.9}$$

$$\& K7 = -85500/(0.02s^2 + 2432.39s + 121569.9)$$

As, $\Delta I_2 = K1\Delta\delta + K2\Delta B_{SVC}$, Gain 3 and Gain 4 are value of $K1$ and $K2$ respectively in figure (5.9). As from equation 8, transfer function 4 and transfer function 3 are value of $K6$ and $K7$ respectively.

BLOCK DIAGRAM

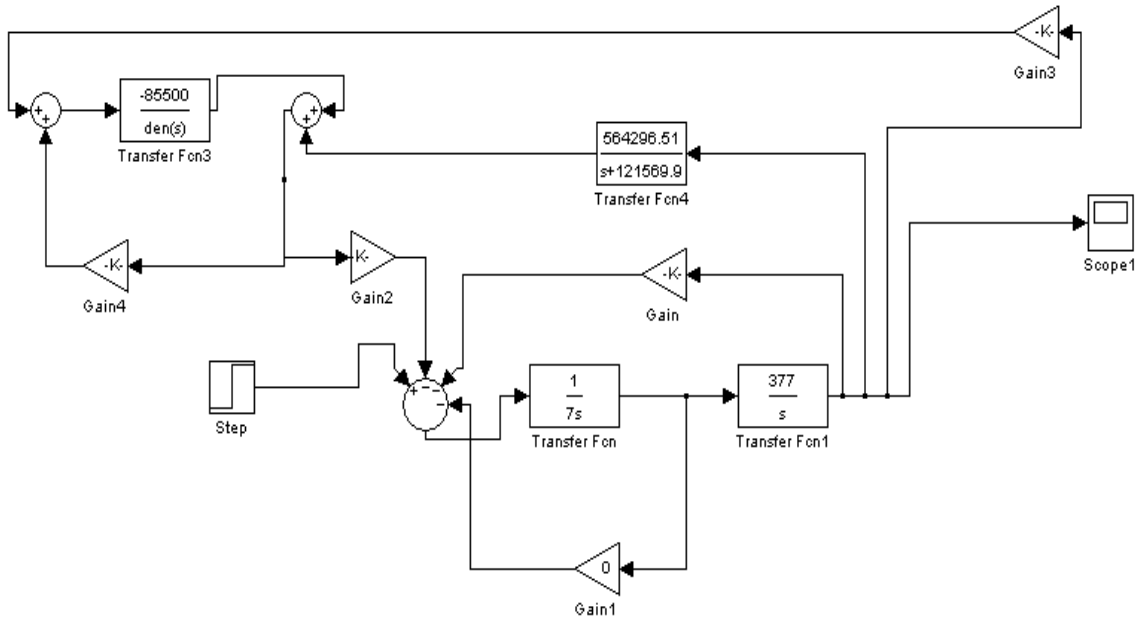


Figure 5.9: SIMULINK modelling of SVC damping controller (line current)

SIMULATION RESULT

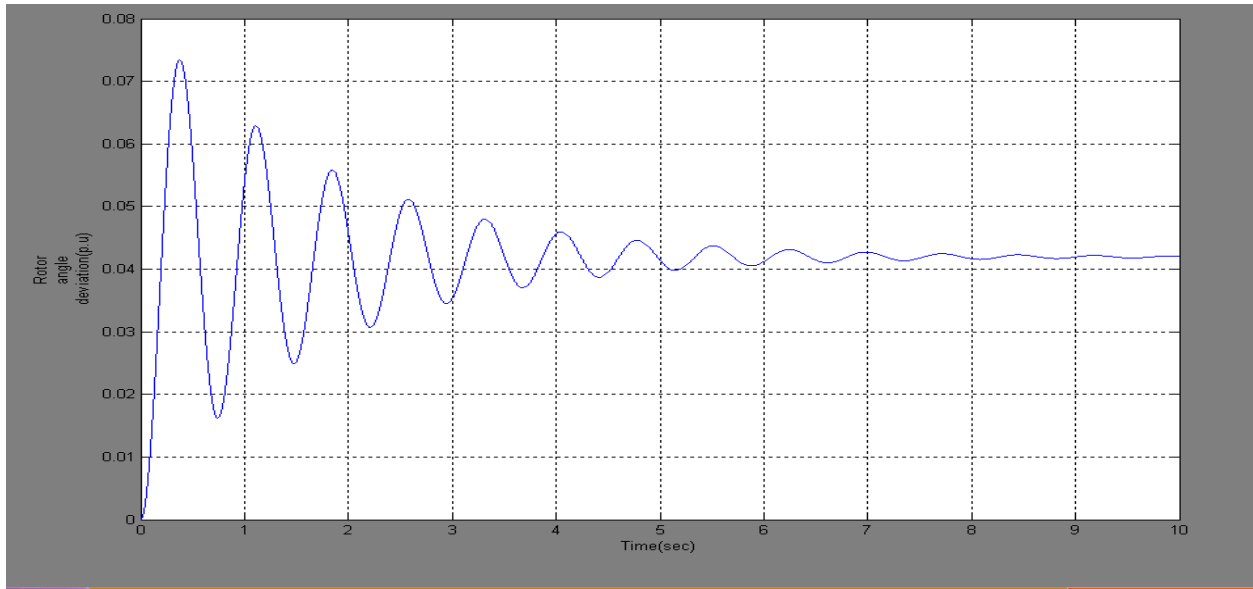


Figure 5.10: Result with line current deviation

State space model of SVC controller using line current as supplementary signal for damping power system oscillation in is prepared and their corresponding block diagram is drawn. Simulation result on MATLAB is given in figure below, which shows a damped system, in which SVC based SMIB unstable system is regaining its original equilibrium point with gradually reducing oscillation to zero value of its amplitude faster than that of the rotor speed as supplementary control signal. So here system is under damping quickly.

SUMMARY-

In a single machine infinite bus system, in which SVC is connected in middle of the transmission line, If any small disturbance make power system oscillatory, oscillation can be damped out using rotor speed and line current both as supplementary signal, but line current signal give better damping of local area mode oscillation as shown in simulation results above. Line current signal as supplementary signal is responding faster in damping the system than rotor speed signal.

5.3: Fuzzy logic based svc controller using different supplementary signal and their simulation results

Under changing operating conditions and uncertainties in system parameters, Fuzzy logic controller is capable of performing better than conventional controller by modulating the output signal of static Var compensator controller.

5.3.1: Fuzzy logic controller with supplementary signal of deviation of rotor Speed.

Fuzzy logic controller is having rotor speed and its derivative as input and Bsvc as its output (susceptance of SVC regulator) is inserted to modulate Bsvc, for this first of all State space model of SVC controller is modified, which is given below.

From fig 1

$$\begin{aligned}
 X_t &= X_d' + X_{trf} + \frac{X_E}{2} \\
 \Rightarrow \quad \vec{I}_1 &= \vec{I}_2 + \vec{I}_3 \\
 \Rightarrow \quad \frac{\vec{E}' - \vec{V}_m}{jX_t} &= \frac{\vec{V}_m - \vec{E}_B}{0.5jX_E} + \vec{V}_m * jB_{SVC} \\
 \vec{V}_m * \left(jB_{SVC} - \frac{j2}{X_E} - \frac{j}{X_t} \right) &= \frac{E' * \cos\delta + E' * j\sin\delta}{jX_t} + \frac{2E_B}{jX_E} \\
 \Rightarrow \vec{V}_m &= \frac{E'X_E\cos\delta + 2E_BX_t}{X_E + 2X_t - X_EX_tB_{SVC}} + j * \frac{E'X_E\sin\delta}{X_E + 2X_t - X_EX_tB_{SVC}}
 \end{aligned}$$

$$let \quad , X = X_E + 2X_t - X_EX_t B_{SVC}$$

$$V_m = \left[\frac{\left\{ (E'X_E\cos\delta + 2X_tE_B)^2 + (E'X_E\sin\delta)^2 \right\}}{\{X\}^2} \right]^{\frac{1}{2}}$$

$$\Rightarrow V_m = f(\delta, B_{SVC})$$

$$\Delta V_m = \left(\frac{\partial V_m}{\partial \delta} \right) * \Delta \delta + \left(\frac{\partial V_m}{\partial B_{SVC}} \right) * \Delta B_{SVC}$$

$$\Delta V_m = - \left[\left\{ \frac{2E'E_B X_E X_t \sin \delta}{V_m * X * X} \right\} \Delta \delta + \left\{ \frac{-V_m X_t X_E}{X} \right\} \Delta B_{SVC} \right] = -[c1 \Delta \delta + c2 \Delta B_{SVC}] \quad \dots \dots (a)$$

From fig 5.2

$$SVC \text{ CONTROLLER} \Rightarrow \Delta B_{SVC} = \frac{Kr}{1 + sTr} \Delta V_m \quad \dots \dots (b)$$

$$\Delta B_{SVC}(1 + sTr) = -Kr(c1 \Delta \delta + c2 \Delta B_{SVC})$$

$$\Delta \dot{B}_{SVC} = \left(\frac{-Kr * c1}{Tr} \right) \Delta \delta - \left(\frac{(1 + Kr * c2)}{Tr} \right) \Delta B_{SVC} \quad \dots \dots (1)$$

ΔTe calculation

$$\vec{I}_2 = \frac{\vec{V}_m - \vec{E}_B}{\frac{jX_E}{2}} = -\frac{j2}{X_E} \left[\left\{ \frac{(E'X_E \cos \delta + 2E_B X_t) + (jE'X_E \sin \delta)}{X} \right\} - E_B \right]$$

$$\overline{(I_2^*)} = \frac{2}{X * X_E} [(E'X_E \sin \delta) + j * (E'X_E \cos \delta + 2E_B X_t - X E_B)]$$

$$in \text{ p.u.}, \quad Pe = Te = real [E_B * \overline{(I_2^*)}] = E_B * \left[\frac{2X_E E' \sin \delta}{XX_E} \right] = \frac{2E'E_B \sin \delta}{X}$$

$$\Delta Te = \left(\frac{\partial Te}{\partial \delta} \right) * \Delta \delta + \left(\frac{\partial Te}{\partial B_{SVC}} \right) * \Delta B_{SVC}$$

$$\frac{2E'E_B \cos \delta}{X} \Delta \delta + \frac{-2E'E_B \sin \delta}{X * X} * (-X_t X_E) \Delta B_{SVC}$$

$$\Delta Te = \left[\frac{2E'E_B \cos \delta}{X} \right] \Delta \delta + \left[\frac{2E'E_B X_t X_E \sin \delta}{X * X} \right] \Delta B_{SVC}$$

$$= c1' \Delta \delta + c2' \Delta B_{SVC} \quad \dots \dots (c)$$

$$\text{where, } c1' = \frac{2E'E_B \cos \delta}{X} \quad \text{and} \quad c2' = \frac{2E'E_B X_t X_E \sin \delta}{X * X}$$

equation of motion with SVC,

$$\Delta \dot{\delta} = w_o * \Delta w_r \quad \dots \dots \dots (2)$$

$$\Delta \dot{w}_r = \frac{\Delta Tm - \Delta Te - K_d \Delta w_r}{2H}$$

$$\Delta \dot{w}_r = \frac{\Delta Tm - (c1' \Delta \delta + c2' \Delta B_{SVC}) - K_d \Delta w_r}{2H} \quad \dots \dots \dots (3)$$

equation 1 & 2 & 3 in vector matrix form,

$$\begin{bmatrix} \Delta \dot{w}_r \\ \Delta \dot{\delta} \\ \Delta \dot{B}_{SVC} \end{bmatrix} = \begin{bmatrix} \frac{-K_d}{2H} & \frac{-c1'}{2H} & \frac{-c2'}{2H} \\ w_o & 0 & 0 \\ 0 & \frac{-K_r c1}{T_r} & -\frac{1+K_r c2}{T_r} \end{bmatrix} \begin{bmatrix} \Delta w_r \\ \Delta \delta \\ \Delta B_{SVC} \end{bmatrix} + \begin{bmatrix} \frac{1}{2H} \\ 0 \\ 0 \end{bmatrix} \Delta Tm$$

... State equation with SVC

laplace transfer of equation (3) gives,

$$\Delta \delta = \frac{w_o}{s} * \left[\frac{\{\Delta Tm - (c1' \Delta \delta + c2' \Delta B_{SVC}) - K_d \Delta w_r\}}{\{2Hs\}} \right] \quad \dots \dots (4)$$

Taking Laplace transform of equation (1) we get,

$$s\Delta B_{SVC} = \frac{-K_r c1}{T_r} \Delta\delta - \frac{1+K_r c2}{T_r} * \Delta B_{SVC}$$

$$\Delta B_{SVC} \left[s + \frac{1+K_r c2}{T_r} \right] = \frac{-K_r c1}{T_r} \Delta\delta$$

$$\Delta B_{SVC} [sT_r + 1 + K_r c2] = -K_r c1 \Delta\delta$$

$$\Delta B_{SVC} = \frac{\left\{ \frac{-K_r c1}{T_r} \right\}}{\left\{ s + \frac{1+K_r c2}{T_r} \right\}} * \Delta\delta = b * \Delta\delta$$

Here transfer fn1 is represented as “b”, gain1 as value of $c1'$ and gain2 as $c2'$ in given block diagram of fig (5.11).

BLOCK DIAGRAM

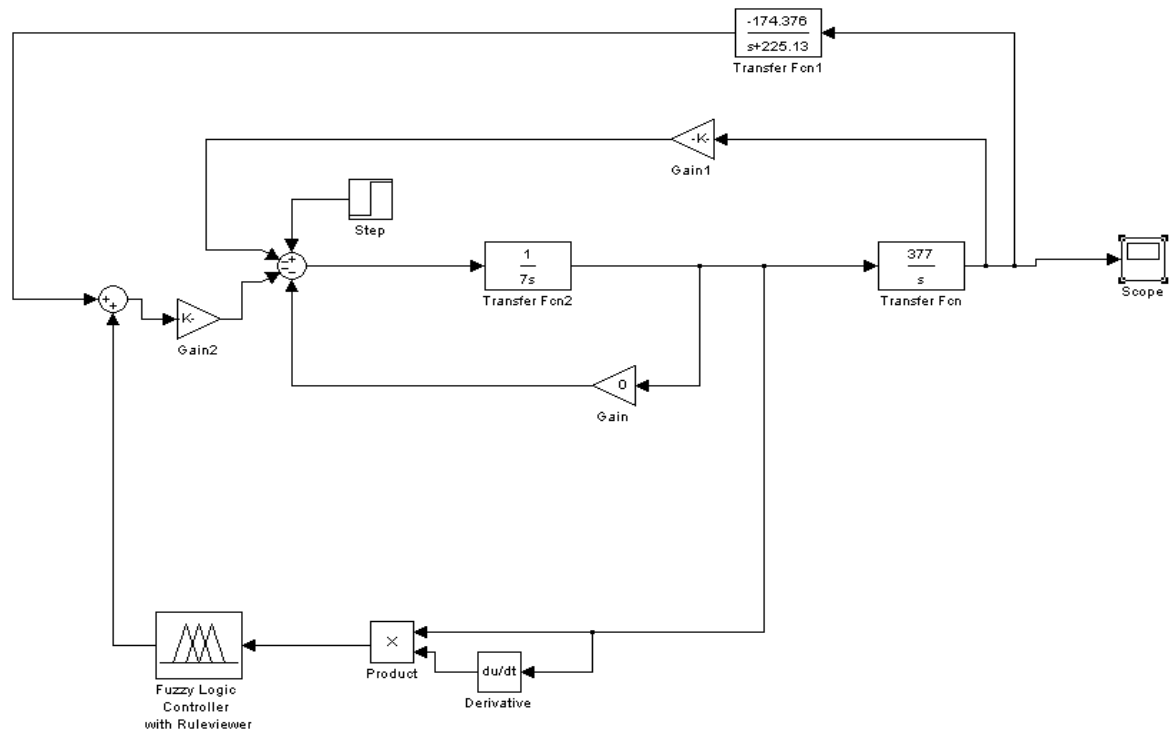


Figure 5.11: SIMULINK modelling of Fuzzy logic based SVC damping Controller (rotor speed)

Fuzzy logic controllers (FLC) are rule-based controllers. The structure of the FLC resembles that of a knowledge based controller except that the FLC utilizes the principles of the fuzzy set theory in its data representation and its logic. The basic configuration of the FLC can be simply represented in four parts.

1. Fuzzification module – the functions of which are first, to read, measure, and scale the control variable (speed, acceleration) and, second, to transform the measured numerical values to the corresponding linguistic (fuzzy variables with appropriate membership values)
2. Knowledge base - this includes the definitions of the fuzzy membership functions defined for each control variables and the necessary rules that specify the control goals using linguistic variables
3. Inference mechanism – it should be capable of simulating human decision making and influencing the control actions based on fuzzy logic
4. Defuzzification module – which converts the inferred decision from the linguistic variables back the numerical values.

Control rules of this Fuzzy logic controller with each of input and output fuzzy variables is assigned five fuzzy subsets varying from negative big to positive big. Each subset is associated with a triangular membership function to form a set of five membership function for each fuzzy variable, result into 25 rules given below-

Δw $/\Delta \dot{w}$	NB	NS	ZE	PS	PB
NB	NB	NB	NB	NS	ZE
NS	NB	NB	NS	ZE	PS
ZE	NB	NS	ZE	PS	PB
PS	NS	ZE	PS	PB	PB
PB	ZE	PS	PB	PB	PB

The typical rules are having the following structure:

Rule 1: If rotor speed deviation is NM (negative medium) and rotor acceleration is PS (positive small) then ΔB_{SVC} , deviation of susceptance of SVC regulator (output of fuzzy logic controller) is NS (negative small).

Rule 2: If rotor speed deviation is NB (negative big) and rotor acceleration is NS (negative small) then ΔB_{SVC} , deviation of susceptance of SVC regulator (output of fuzzy logic controller) is NB (negative big).

Rules are formed on the basis of the knowledge that as rotor angle increases, rotor speed deviation becomes positive. To make this deviation to a zero value (i.e damping power system oscillation), we need to increase the input electrical power (P_e) and so to increase the B_{SVC} (susceptance of SVC).

Simulation result on MATLAB is given in figure below, which shows a damped system, in which SVC based SMIB unstable system is regaining its original equilibrium point with gradually reducing oscillation to zero value of its amplitude. So here system is under damped.

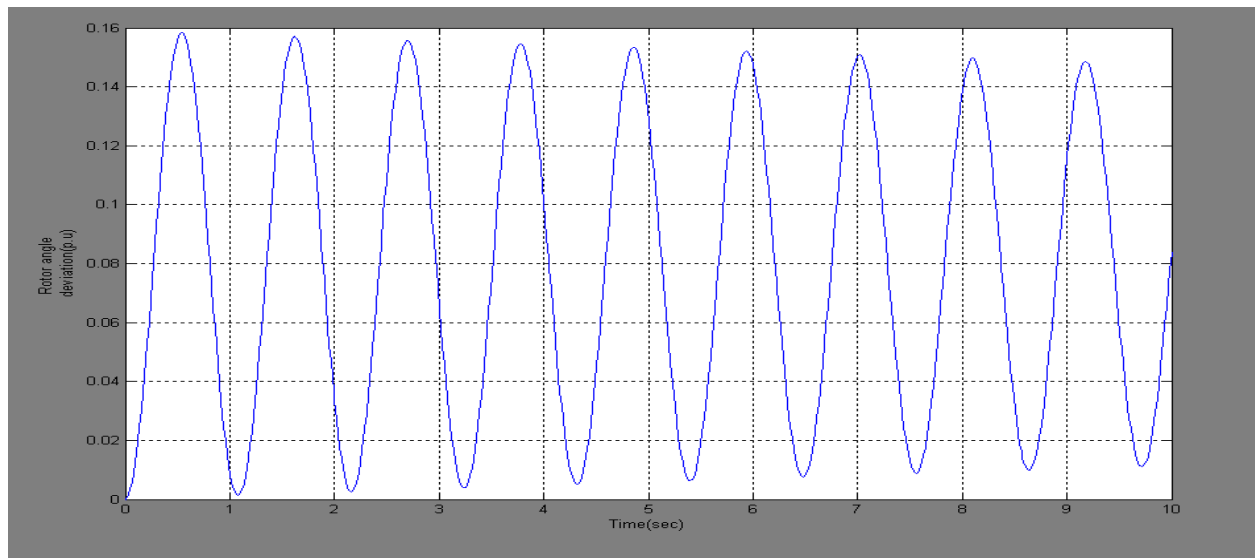


Figure 5.12: Result with rotor speed deviation

5.3.2: Fuzzy logic controller with supplementary signal of deviation of bus Voltage.

Fuzzy logic controller is having bus voltage ΔV_m and its derivative as input and Bsvc as its output (susceptance of SVC regulator) is inserted to modulate Bsvc signal, for this State space model of SVC controller is modified as shown in block diagram of fig (5.13). As it is derived above,

$$\Delta V_m = -\left[\left\{\frac{2E'E_B X_E X_t \sin \delta}{V_m * X * X}\right\} \Delta \delta + \left\{\frac{-V_m X_t X_E}{X}\right\} \Delta B_{SVC}\right]$$

$$= -[c1 \Delta \delta + c2 \Delta B_{SVC}].$$

I.e Bus voltage is function of $\Delta \delta$ and ΔB_{SVC} signal. With the help of gain block, Gain3 and Gain4, input signal for Fuzzy logic controller is taken and now modified output Bsvc is given back to gain block, Gain2 as shown in block diagram of fig(5.13). Simulation result on MATLAB shows a damped system. In the block diagram of fig (5.13), Gain3= c2 & Gain4= -c1

BLOCK DIAGRAM

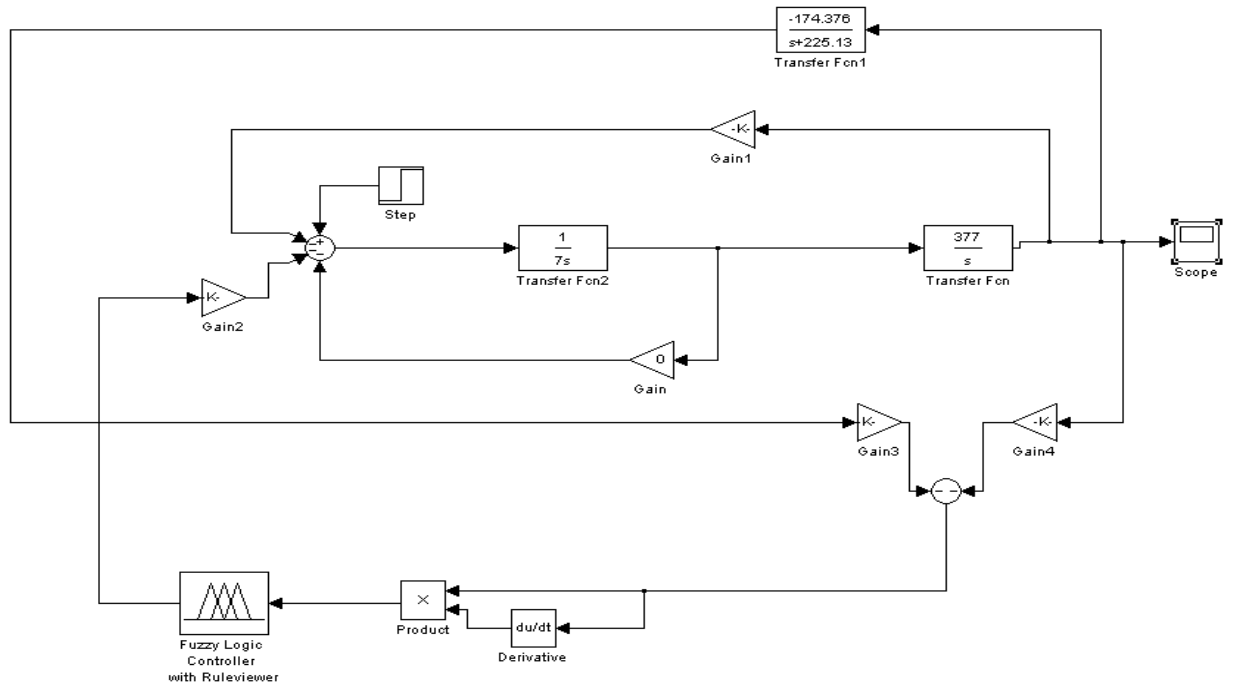


Figure 5.13: SIMULINK modelling of Fuzzy logic based SVC damping Controller (bus voltage)

Control rules with each of input and output fuzzy variables is assigned seven fuzzy subsets varying from negative big to positive big. Each subset is associated with a triangular membership function to form a set of seven membership function for each fuzzy variable, result into 49 rules given below.

$\Delta \dot{V}_m / \Delta V_m$	NB	NM	NS	ZE	PS	PM	PB
NB	NB	NB	NB	NB	NM	NS	ZE
NM	NB	NB	NB	NM	NS	ZE	PS
NS	NB	NB	NM	NS	ZE	PS	PM
ZE	NB	NM	NS	ZE	PS	PM	PB
PS	NM	NS	ZE	PS	PM	PB	PB
PM	NS	ZE	PS	PM	PB	PB	PB
PB	ZE	PS	PM	PB	PB	PB	PB

The typical rules are having the following structure:

Rule 1: If bus voltage deviation is NM (negative medium) and derivative of bus voltage deviation is PS (positive small) then ΔB_{SVC} , deviation of susceptance of SVC regulator (output of fuzzy logic controller) is NS (negative small).

Rule 2: If bus voltage deviation is NM (negative medium) and derivative of bus voltage deviation is PB (positive big) then ΔB_{SVC} , deviation of susceptance of SVC regulator (output of fuzzy logic controller) is PS (positive small).

Rules are formed as shown in fig (e) that with the increase of rotor angle, bus voltage magnitude decreases. Thus bus voltage deviation becomes negative and so from fig (5.2), ΔB_{SVC} also become negative. To make this deviation to a zero value, we need to increase the B_{SVC} (susceptance of SVC).

Simulation result on MATLAB is given in figure below, which shows a damped system, in which SVC based SMIB unstable system is regaining its original equilibrium point with gradually reducing oscillation to zero value of its amplitude faster in this case. So here system is under damped also bus voltage signal is proved to be better than rotor speed deviation signal for Fuzzy logic controller to damp the power system oscillation.

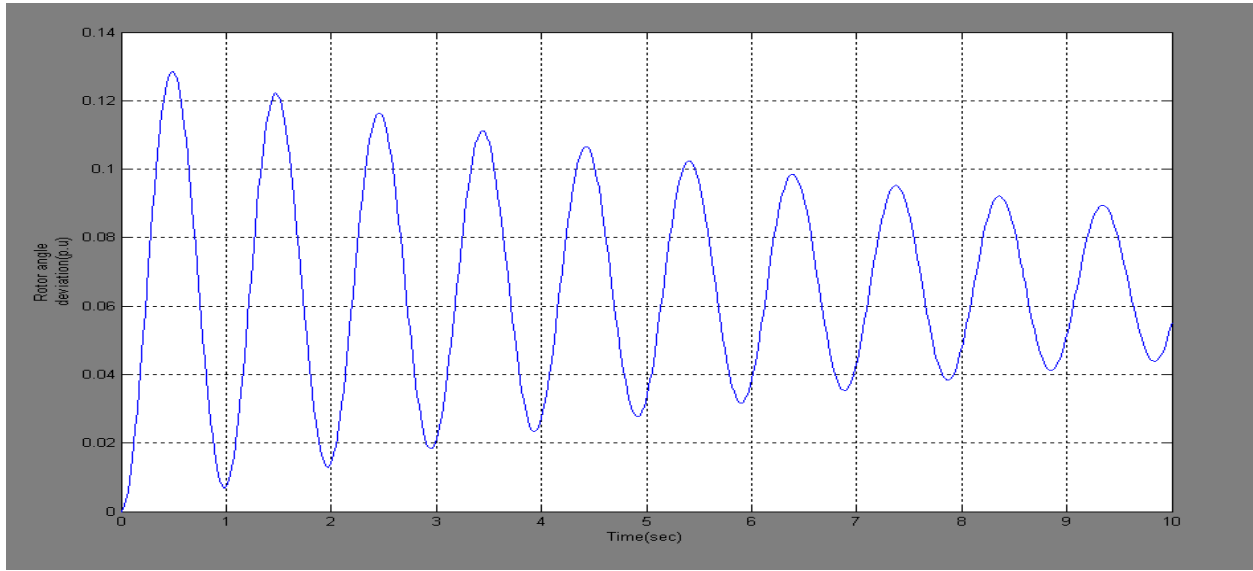


Figure 5.14: Result with bus voltage deviation

5.3.3: Fuzzy logic controller with supplementary signal of deviation of line current

Fuzzy logic controller is having line current ΔI_2 and its derivative as input and B_{svc} as its output (susceptance of SVC regulator) is inserted in state space model of SVC controller to modulate B_{svc} signal, As it is derived above,

$$\Delta I_2 = K1\Delta\delta + K2\Delta B_{svc}$$

I.e line current is function of $\Delta\delta$ and ΔB_{svc} signal. With the help of gain block, Gain3 and Gain4 input signal for Fuzzy logic controller is taken and thus now modified output B_{svc} is given back to gain block, Gain2 as shown in block diagram of fig(5.15). Simulation result on MATLAB shows a damped system. In the block diagram given below Gain3= $K1$ & Gain4= $K2$

BLOCK DIAGRAM

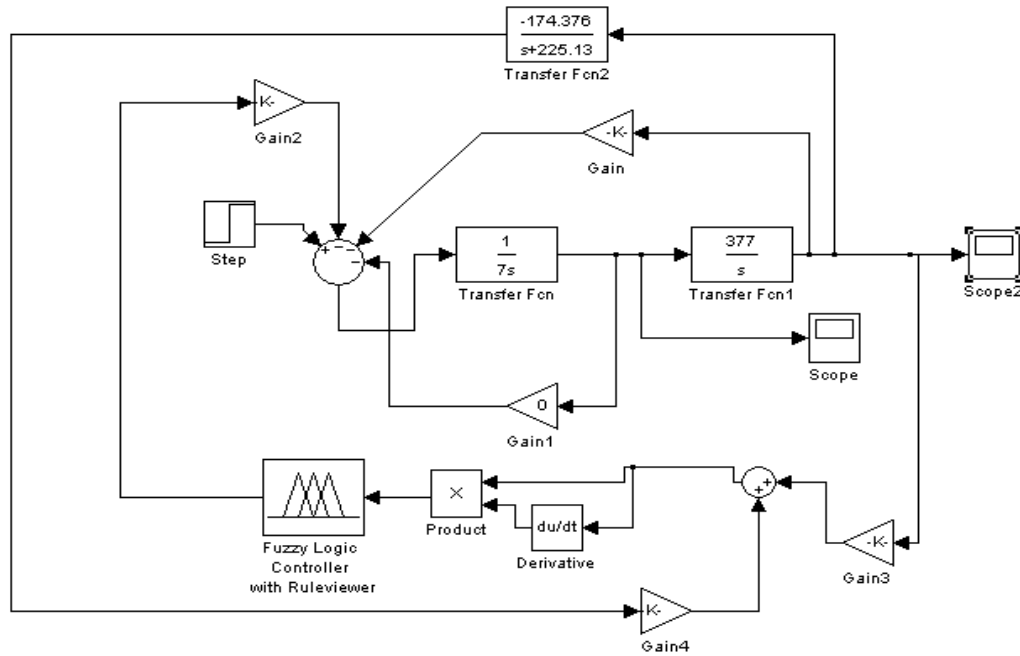


Figure 5.15: SIMULINK modelling of Fuzzy logic based SVC damping Controller (line current)

Control rules with each of input and output fuzzy variables is assigned five fuzzy subsets varying from negative big to positive big. Each subset is associated with a triangular membership function to form a set of five membership function for each fuzzy variable result into 25 rules given below-

$\Delta I_2/\Delta \dot{I}_2$	NB	NS	ZE	PS	PB
NB	NB	NB	NB	NS	ZE
NS	NB	NB	NS	ZE	PS
ZE	NB	NS	ZE	PS	PB
PS	NS	ZE	PS	PB	PB
PB	ZE	PS	PB	PB	PB

The typical rules are having the following structure:

Rule 1: If line current deviation is NB (negative big) and derivative of it is PS (positive small) then ΔB_{SVC} , deviation of susceptance of SVC regulator (output of fuzzy logic controller) is NS (negative small).

Rule 2: If bus voltage deviation is NS (negative small) and derivative of it is PB (positive big) then ΔB_{SVC} , deviation of susceptance of SVC regulator (output of fuzzy logic controller) is PS (positive small).

Rules are structured on the basis that with the increase of rotor angle, line current magnitude increases. Thus deviation of line current become positive and so ΔB_{SVC} . To make this deviation to a zero value, we need to decrease the B_{SVC} (susceptance of SVC).

Simulation result on MATLAB is given in figure below, which shows a damped system. With fuzzy logic controller, Line current as a supplementary signal gives better response in power oscillation damping than bus voltage and rotor speed deviation. Critical damping is achieved with line current as supplementary signal as shown in fig(5.16). However this is not the case with bus voltage and rotor speed deviation signals

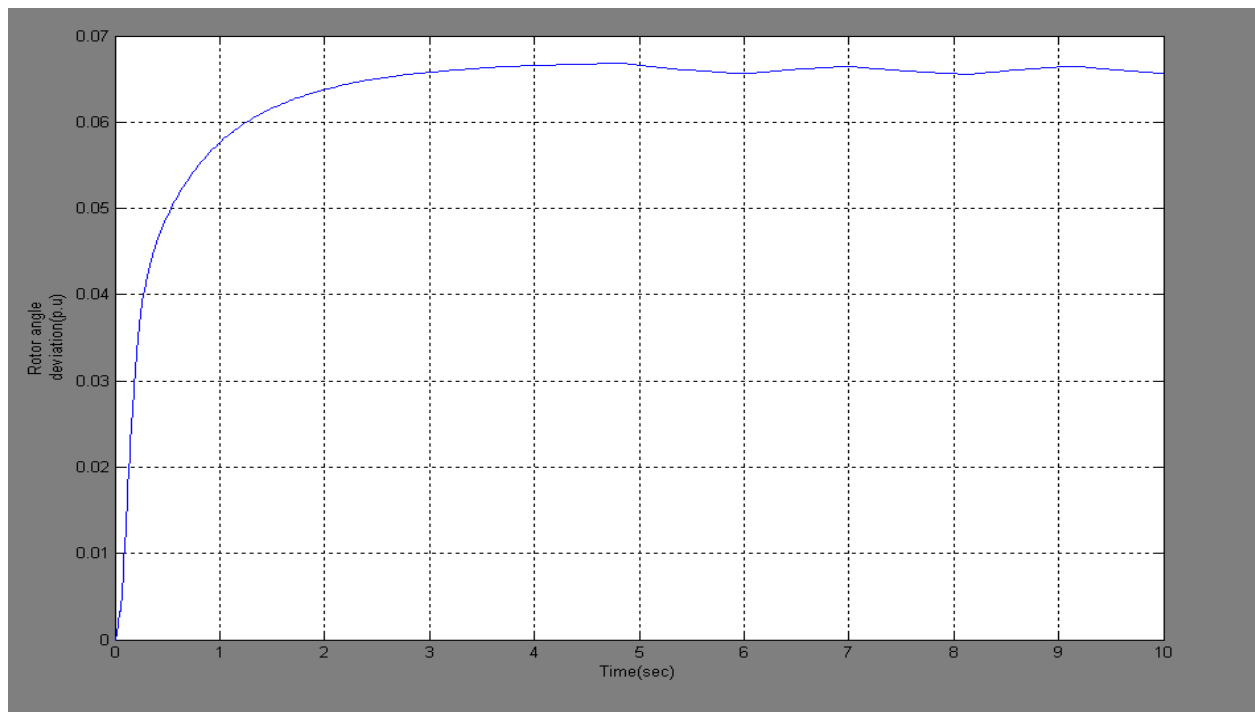


Figure 5.16: Result with line current deviation

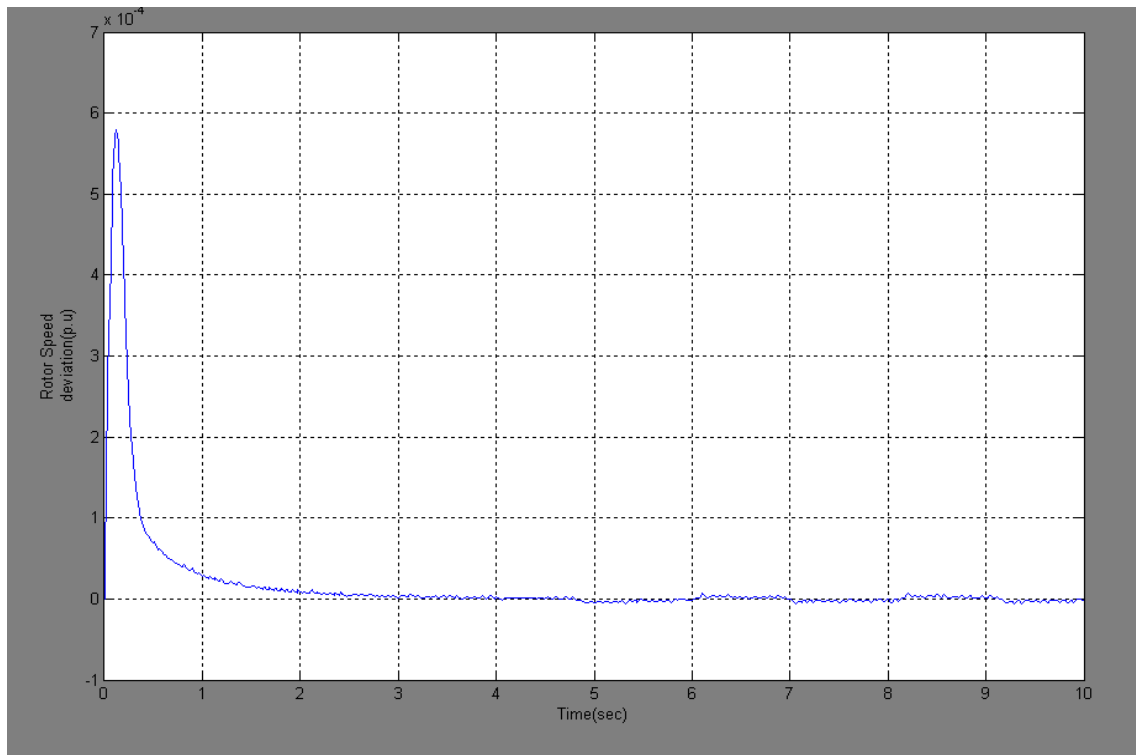


Figure 5.16: Result with line current deviation

CONCLUSIONS AND SCOPE OF FUTURE WORK

State space modelling of SVC damping controller with supplementary signals in a single machine infinite bus system is presented for the purpose of damping the low frequency oscillations and subsequently, a Fuzzy logic controller has been implemented to enhance the performance. Fuzzy logic controller shows faster response than conventional controller in damping power system oscillation. MATLAB simulation validates the above.

With fuzzy logic controller, line current as a supplementary signal gives better response in power oscillation damping than bus voltage and rotor speed deviation. Also, bus voltage signal shows better response than rotor speed signal. Critical damping is achieved with line current as supplementary signal. However this is not the case with bus voltage and rotor speed deviation signals.

Among all the three supplementary control signals, line current signal is more effective for power oscillation damping vis-à-vis both conventional and fuzzy logic controller.

No of control rules in rule base can be extended to improve the performance of the fuzzy logic based damping controller. Combination of two supplementary signals can be used to improve the damping.

OBSERVABILITY and CONTROLLABILITY with different supplementary control signals can be compared for better performance characteristic.

REFERENCES

1. Power system stability and Control 'Prabha Kundur'. Copyright 1994, third reprint 2007, Tata McGraw hill.
2. Kundur, P., Paserba, J., Ajarapu, V., Andersson, G., Bose, A., Canizares, C., Hatziargyriou, N., Hill, D., Stankovic, A., Taylor, C., Van Cutsem, T., Vittal, V. "Definition and classification of power system stability" 2004, IEEE/CIGRE joint task force on stability terms and definitions Power Systems, IEEE Transactions on Volume: 19, Issue: 3, pp. 1387 - 1401
3. S.B Cray "Power system stability" John Wiley & Sons, Inc., 1955, Vol.II.
4. Murdoch, A., Venkatarman, S., Sanchez-Gasca, J.J., Lawson, R.A. "Practical application considerations for power system stabilizer (PSS) controls" 1999, Power Engineering Society Summer Meeting, 1999. IEEE Volume: 1. pp. 83 - 87 vol.1.
5. Xue Wu, Li Wenyun, Cao Kunnan, Zhao Yun "Improvement of dynamic stability of Yunnan Province and South-China power system by power system stabilizer (PSS)" 2000, Power System Technology, 2000. Proceedings. Power con 2000. International Conference on Volume: 3. pp. 1179 - 1183 vol.3.
6. Safie, S.I., Majid, M.S., Hasimah, A.R., Wahab, A., Yusri, H.M. "Sliding mode control power system stabilizer (PSS) for Single Machine Connected to Infinite Bus (SMIB)" 2008 Power and Energy Conference, 2008. PECON2008. IEEE 2nd International. pp. 122 - 126.
7. O'Brien, M., Ledwich, G. "Static reactive-power compensator controls for improved system stability" 1987. Generation, Transmission and Distribution, IEE Proceedings C. Volume: 134, Issue: 1. pp. 38 - 42.
8. Aboul-Ela, M.E., Sallam, A.A., McCalley, J.D., Fouad, A.A. "Damping controller design for power system oscillations using global signals" 1996. Power Systems, IEEE Transactions Volume: 11, Issue: 2. pp. 767 - 773.
9. El-Emary, A.A. "Formula for the effect of a static Var compensator on synchronizing torque coefficient" 1996. Generation, Transmission and Distribution, IEE Proceedings Dept. of Electrical. Power & Machines, Cairo Univ., Giza vol.143, Issue: 6, pp. 582 - 586.
10. Y.L.Tan, Y Wang, "Effects of FACTS controller line compensation on Power System Stability" Power Engineering Review IEEE, 1998, pp 55-56.
11. Castro, M.S.; Nassif, A.B.; da Costa, V.F.; da Silva, L.C.P. "Impacts of FACTS controllers on damping power systems low frequency electromechanical oscillations" 2004. Transmission and Distribution Conference and Exposition: Latin America, 2004 IEEE/PES. pp. 291-296.
12. Gelen, A.; Yalcinoz, T. "The Behavior of TSR-based SVC and TCR-based SVC Installed in an infinite bus system" IEEE 2008, pp 120-124.

13. Dr.V.K.Chandrakar, Prof.S.N.Dhurvey, Mr.S.C.Suke,"Performance comparison of SVC with POD and PSS for Damping of Power System Oscillations" Emerging trends in engineering and technology(ICETET),2010 3rd international conference . pp 247-252.
14. Therattil, J.P., Panda, P.C. "Dynamic stability enhancement using self-tuning Static Var Compensator" 2010, India Conference (INDICON), 2010 Annual IEEE. Pp. 1 – 5.
15. Ghazanfar Shahgholian, Seyed Mohsen Mirbagheri, Hosein Safaeipoor, Mehdi Mahdavian, "The Effect of SVC-FACTS controller on power system oscillation damping control" 2011 IEEE, pp 1-5.
16. Omelkhir Yahyaoui , Raouia Aquini , Khadija Benkilani, Mohamed Elleuch" Enhancement of voltage stability in ultra high voltage electric network by Static Var Compensation" 2011 IEEE, 8th International Multi-conference on system, signal & devices. pp 1-6.
17. Pravin Chapadel, Dr.Marwan Bikdas, Dr.Ibraheem kateeb, Dr.Ajit D.Kelkar,"Reactive Power management and voltage control of large Transmission system using SVC (Static VAR Compensator).2011 IEEE. Pp 85-90.
18. Shahgholian, G.; Mirbagheri, S.M.; Safaeipoor, H.; Mahdavian, M."The effect of SVC-FACTS controller on power system oscillation damping control "2011. Electrical Machines and Systems (ICEMS), 2011 International Conference .pp. 1 – 5.
19. Dash, P.K., Mishra, S., Liew, A.C" Fuzzy", Generation, Transmission and Distribution, 1995IEEE Proceedings- Volume: 142, Issue: 6 pp. 618 – 624.
20. Nair, M.G.; Nambiar, T.N.P."Fuzzy logic based FACTS controller for damping oscillations "2002.Transmission and Distribution Conference and Exhibition 2002: Asia Pacific. IEEE/PES Volume: 3. pp. 2019 - 2022 vol.3.
21. Khan, L.; Rogers, G.J.; Lozano, C.A." Intelligent control of FACTS for damping power system low frequency oscillations ", 2004. Multitopic Conference, 2004. Proceedings of INMIC 2004. 8th International .pp. 731 – 736.
22. Kazemi, A.; Sohrforouzani, M.V." A. Power system damping using fuzzy controlled FACTS devices ", 2004.Power System Technology, 2004. PowerCon2004. 2004 International Conference. pp. 1623-1628, vol: 2
23. Ramirez-Gonzalez, M., Malik, O.P., "Simplified Fuzzy Logic Controller and Its Application as a Power System Stabilizer"2009, Intelligent System Applications to Power Systems, 2009. ISAP '09.15th International Conference. pp. 1 – 6.
24. Roosta, A.R., Khorsand, H., Nayeripour, M. "Design and analysis of fuzzy power system stabilizer "2010, Innovative Smart Grid Technologies Conference Europe (ISGT Europe), 2010 IEEE PES. pp. 1-7
25. Hosseini, S.M.H. Olamaee, J. ; Samadzadeh, H. "Power oscillations damping by Static Var Compensator using an Adaptive Neuro-Fuzzy controller "2011 Electrical and Electronics Engineering (ELECO), 2011 7th International Conference . pp. 1-80 - 1-84.

26. Patel, H.D., Majmudar, C. "Fuzzy logic application to single machine power system stabilizer "2011, Engineering (NUICONE), 2011 Nirma University International Conference. pp. 1 – 6
27. Renuka, T.K.; Manakkal, S."A tuned fuzzy based power system stabilizer for damping of Low Frequency Oscillations"2012. Power, Signals, Controls and Computation (EPSCICON), 2012 International Conference .pp. 1-6.